

Secure Key from Quantum Discord

Rong Wang,^{1,*} Guan-Jie Fan-Yuan,^{2,3,4,†} Zhen-Qiang Yin,^{2,3,4,‡} Shuang Wang,^{2,3,4,§}
Hong-Wei Li,⁵ Yao Yao,⁶ Wei Chen,^{2,3,4} Guang-Can Guo,^{2,3,4} and Zheng-Fu Han^{2,3,4}

¹*Department of Physics, University of Hong Kong, Pokfulam Road, Hong Kong SAR, China*

²*CAS Key Laboratory of Quantum Information, University of Science and Technology of China, Hefei 230026, China*

³*CAS Center for Excellence in Quantum Information and Quantum Physics,
University of Science and Technology of China, Hefei 230026, China*

⁴*Hefei National Laboratory, University of Science and Technology of China, Hefei 230088, China*

⁵*Henan Key Laboratory of Quantum Information and Cryptography,*

Zhengzhou Information Science and Technology Institute, Henan, 450000, Zhengzhou, China

⁶*Microsystems and Terahertz Research Center, China Academy of Engineering Physics, Chengdu Sichuan 610200, China*

The study of quantum information processing seeks to characterize the resources that enable quantum information processing to perform tasks that are unfeasible or inefficient for classical information processing. Quantum cryptography is one such task, and researchers have identified entanglement as a sufficient resource for secure key generation. However, quantum discord, another type of quantum correlation beyond entanglement, has been found to be necessary for guaranteeing secure communication due to its direct relation to information leakage. Despite this, it is a long-standing problem how to make use of discord to analyze security in a specific quantum cryptography protocol. Here, based on our proposed quantum discord witness recently, we successfully address this issue by considering a BB84-like quantum key distribution protocol and its reduced entanglement-based version. Our method is robust against imperfections in qubit sources and qubit measurements as well as basis misalignment due to quantum channels, which results in a better key rate than standard BB84 protocol. Those advantages are experimentally demonstrated via photonic phase encoding systems, which shows the practicality of our results.

I. INTRODUCTION

Over the last three decades, quantum resources [1] and their role in quantum information processing have been the subject of significant research. One key task that has garnered particular interest is quantum key distribution (QKD) [2], which is used to generate secure cryptographic keys between two remote parties based on the principles of quantum physics. QKD has seen considerable progress both in theory and practice [3–12] and is slated for industrial applications. Since QKD has a such appealing characteristic, it is natural to think about what kind of resource and how much do people need to guarantee security. The ability of entanglement distillation can guarantee both the correctness and the secrecy [3, 4, 13–17], so that entanglement is widely recognized as a crucial resource. However, an important question remains: if solely looking at the secrecy in QKD, do any other factors contribute to it?

As an alternative, in Ref. [18], Pirandola first proposed the point that quantum discord (QD) [19, 20], which characterizes the quantum correlation beyond entanglement, can be viewed as a resource for the secrecy in QKD protocols. However, it is not clear what resulting key rate one may get and thus whether a formulation using QD is of any practical interest. As well, it

is not clear what the advantages are by using QD, either. In this paper, we first introduce a BB84-like protocol which can be grouped into the prepare-and-measure (PM) category, and we shall prove that there exists a reduced entanglement-based (EB) version of this protocol. Based on this EB version, we then study a specific case of the connection between information leakage and QD, which has been firstly studied in Pirandola’s work [18].

Benefiting from our recently proposed QD witness [21], we propose a general security framework against collective attack by directly linking the information leakage to our QD witness. Following the security proof of our proposed protocol, we go one step deeper to understand the role of QD behind the protocol and answer the question that QD, capturing entanglement as a subset, is in fact the necessary resource in our scenario. Therefore, we call our protocol discord-based (DB) QKD. Besides the fundamental study of understanding the role of QD in QKD, by employing the photonic phase encoding systems, we experimentally show the advantages of QD at a practical level. Based on the essential feature of our QD witness, we can overcome the imperfect qubit-based processes such as imperfect qubit preparation [22–24]. More concisely, in our physical model, we allow uncharacterized qubit preparation and qubit measurement, which is absolutely beyond the assumption of standard BB84 protocol. Therefore, our theory significantly reduces the requirements for the real-world devices. Another surprising thing, our QD witness shows rotation invariance so that DB-QKD is tolerable for the misalignment, which suggests a better key rate than standard BB84 protocol.

* rwangphy@hku.hk

† The author contributes equally as the first author.

‡ yinzq@ustc.edu.cn

§ wshuang@ustc.edu.cn

II. QUANTUM DISCORD WITNESS

QD is defined by the difference between two different mutual information calculated from a bipartite quantum state ρ_{AB} within the Hilbert space $\mathcal{H}_A \otimes \mathcal{H}_B$. One of the mutual information is defined by $I(A : B) = H(A) + H(B) - H(AB)$, where $H(\cdot)$ is the Von Neumann entropy, the other one is defined by $J(B|A) = H(B) - \min_{\{E_a\}} H(B|E_a)$ where $H(B|E_a)$ is the conditional entropy for the post-measurement state $\rho'_{AB} = \sum_a M_a \rho_{AB} M_a^\dagger$ described by the positive operator-valued measure (POVM) with elements $E_a = M_a^\dagger M_a$ on \mathcal{H}_A . $I(A : B)$ is understood as the amount of total correlations [25] and $J(B|A)$ is viewed as the contribution of its classical part, so that the part of quantum correlation is given by

$$\begin{aligned} D(B|A) &= I(A : B) - J(B|A) \\ &= \min_{\{E_a\}} H(B|E_a) + H(A) - H(AB), \end{aligned} \quad (1)$$

where the minimization is over all POVMs $\{E_a\}$.

Inspired by dimension witness in a prepare-and-measure scenario with independent devices [26], we recently proposed a QD witness [21] with uncharacterized devices, and briefly review it here. It says that for any unknown two-qubit state ρ_{AB} separately retained by two parties named Alice and Bob, Alice (Bob) randomly chooses $x \in \{0, 1\}$ ($y \in \{0, 1\}$) performs an unknown two-dimensional POVM A_x (B_y) on her (his) qubit and obtains the outcome $a \in \{0, 1\}$ ($b \in \{0, 1\}$). Then, Alice and Bob compute the expectation values $\langle A_x \rangle = \Pr[a = 0|x] - \Pr[a = 1|x] = \text{Tr}[\rho_A A_x]$, $\langle B_y \rangle = \Pr[b = 0|y] - \Pr[b = 1|y] = \text{Tr}[\rho_B B_y]$ and $\langle A_x \otimes B_y \rangle = \Pr[a = b|xy] - \Pr[a \neq b|xy] = \text{Tr}[\rho_{AB} A_x \otimes B_y]$, where ρ_A and ρ_B are respectively the subsystem of Alice and Bob. We have defined the quantity $Q_{xy} = \langle A_x \otimes B_y \rangle - \langle A_x \rangle \langle B_y \rangle$, and then the QD witness is given by [21]

$$W = \begin{vmatrix} Q_{00} & Q_{01} \\ Q_{10} & Q_{11} \end{vmatrix}. \quad (2)$$

In the reduced EB version of DB-QKD, we shall prove that ρ_{AB} shared by Alice and Bob is a two-qubit Bell-diagonal state, and its Bloch representation is

$$\rho_{AB} = \frac{1}{4}(I \otimes I + T_x \sigma_x \otimes \sigma_x + T_y \sigma_y \otimes \sigma_y + T_z \sigma_z \otimes \sigma_z), \quad (3)$$

where I is the identity matrix, σ_x , σ_y and σ_z are the three Pauli matrices, T_x , T_y and T_z with the order $|T_z| \geq |T_x| \geq |T_y|$ are the coefficients. Actually, if the primitive sequence is not that case, we can reorder it by some local unitary operations on both sides. For the Bell-diagonal state with the described order, it has been proved that $W_{\max} = |T_z T_x|$ (see Eq. (10) in [21]), and we here go one step further to show that the lower bound of QD in Eq. (1) is

$$D(B|A) \geq 1 - h\left(\frac{1 - W_{\max}}{2}\right), \quad (4)$$

where $h(\cdot)$ denotes the binary entropy function, W_{\max} is the maximal achievable witness over all POVMs of both Alice and Bob. The detailed proof of all claims above can be found in the Supplementary Materials.

III. PROTOCOL DESCRIPTION

Before proposing our main result, we describe the protocol steps of DB-QKD, which is quite similar to qubit-based BB84 protocol. And then we discuss the assumptions in our protocol. The protocol runs as Tab. I shows.

TABLE I. **The actual protocol**

-
- **State preparation:** In each round, Alice randomly chooses a basis value $x \in \{0, 1\}$, and chooses a uniformly random bit value $a \in \{0, 1\}$ as her raw data. The source is expected to accordingly prepare qubit states $\{|0\rangle, |1\rangle, |+\rangle, |-\rangle\}$, but actually prepare uncharacterized qubit states $\{\tau_{x,a}\}$.
 - **Distribution:** In each round, Alice sends the quantum state to Bob through the insecure channel.
 - **Modulation:** In each round, Bob uniformly at random chooses a modulation value $z \in \{0, 1\}$. The modulator is expected to accordingly modulate the qubit with operations $\{\mathcal{I}, \mathcal{Y}\}$, but actually perform uncharacterized modulations $\{\mathcal{G}_z\}$, where \mathcal{I} and \mathcal{Y} respectively correspond to identity map and σ_y map.
 - **Measurement:** In each round, Bob randomly chooses a basis value $y \in \{0, 1\}$. Measurement device is expected to accordingly measure the qubit in the basis $\{\mathbb{Z}, \mathbb{X}\}$, but actually perform an uncharacterized two-outcome POVMs $\{N_y\}$, and then, outputs a bit value $c \in \{0, 1\}$. Bob takes $b := c \oplus z$ as his raw key.
 - **Parameter estimation:** Alice and Bob publicly announce a part of their raw data and calculate the bit error e_{xy} for each basis combination (x, y) . If the secret key rate calculated from these distributions is positive, then continue the protocol, if not, abort the protocol.
 - **Key generation:** Alice and Bob keep the leftover data of $x = y = 0$ for the final secure key extraction.
 - **Post-processing:** Alice and Bob perform a direct information reconciliation including error correction and privacy amplification to obtain the final secret key.
-

Based on above descriptions, we list the assumptions that are required in this protocol. (1).–The devices are trusted but imperfect. Thus, Eve does not have any prior information about the basis value x , Alice's bit value a , modulation value z and the basis value y . And the source, modulator and measurement device are independent [26]. (2).–The states $\{\tau_{x,a}\}$, modulations $\{\mathcal{G}_z\}$ and measurements $\{N_y\}$ are independently and identically distributed (i.i.d) in each round. (3).–The loss caused by modulator is independent of the incoming state and the choice of modulation value z . The detection efficiency is independent of the choice of measurement basis y . (4).– $\{\tau_{x,a}\}$ are qubit states, $\{\mathcal{G}_z\}$ are qubit modulations i.e. completely-

positive trace preserving (CPTP) maps, and $\{N_y\}$ are two-dimensional POVMs.

Before proceeding, there are several remarks on potential gaps between these theoretical assumptions and practical implementation. For assumption (1), the imperfection means that the forms of qubit states $\{\tau_{x,a}\}$, qubit modulation and qubit measurement are unknown to users. We stress that Eve may know the specific forms of them, but she cannot change them. The independence in assumption (1) means the quantum state preparation, the modulation and measurement have no pre-shared resources, which implies that prepared quantum states $\{\tau_{x,a}\}$, the CPTP maps $\{\mathcal{G}_z\}$ and measurements $\{N_y\}$ only depend each one's local input. For assumption (3), one may argue that since the qubit modulations $\{\mathcal{G}_z\}$ in practice are usually performed by using linear optical systems, they are always lossy. Evidently, provided this loss is independent to the values of $\{x,a\}$ and y , the security proof here holds. Indeed, for a linear optical modulation system, it's often believed that it may adsorb a photon with a certain probability which is not or very weakly related to the quantum state of the incoming photon and modulation parameter z . In this view, the loss owing to the qubit modulations $\{\mathcal{G}_z\}$ is viewed as part of channel loss, and thus $\{\mathcal{G}_z\}$ are treated as CPTP maps, as assumed in assumption (4). Similarly, the measurement loss due to inefficiency of detectors are also viewed as part of channel loss. Finally, assumption that measurement are two-dimensional could be removed by using techniques introduced in [27, 28], which is quite similar to the case of loss-tolerant QKD protocol [22]. Albeit the quit assumption of $\{\tau_{x,a}\}$, weak phase-randomized coherent state is applicable with the help of decoy-state method [29–32]. In a word, the assumptions made here are relevant for typical QKD implementations, in which the devices are imperfect but not malicious.

IV. SECURITY ANALYSIS

In this section, we present our main result and a sketch proof, one can refer to Supplementary Materials for full proof. Since our protocol is based on PM scenario, we shall modify our QD witness from EB version to PM version and defined as the following determinant,

$$W = \begin{vmatrix} 1 - 2e_{00} & 1 - 2e_{01} \\ 1 - 2e_{10} & 1 - 2e_{11} \end{vmatrix}, \quad (5)$$

where e_{xy} is the bit error of basis combination (x,y) . From the viewpoint of security proof of QKD, QD witness is a useful quantity for several reasons. First, it makes use of the statistics from rejected data [33] to bound the eavesdropper, Eve's information. In contrast, the standard BB84 protocol only uses the data sent and received in the same basis to detect Eve. As suggested in [33], rejected data that are sent and received in different basis can be useful for detecting eavesdroppers. Second,

W is robust to imperfections [21]. Provided the preparation and measurements are done on qubits, the actual operator used in the preparation and measurement can be uncharacterized without compromising its calculation. This is a remarkable feature. In contrast, the standard BB84 protocol assumes that either the state preparation or measurement operators are perfect, if not both [34]. In the asymptotic scenario, the secret key rate against collective attack is given by

$$R \geq 1 - h(Q) - h\left(\frac{1-W}{2}\right), \quad (6)$$

where $Q = e_{00}$ is the bit error for key generation basis, and we omit the sifting factor.

Before security proof, we reduce the measurements $\{N_y\}$ to projective measurements $\{B_y\}$. To this end, we first reduce the procedure from measurements $\{N_y\}$ proceeded by modulations $\{\mathcal{G}_z\}$ to restricted measurements $\{M_y\}$ proceeded by *one* channel, denoted by \mathcal{G} . This reduction actually follow the idea that quantum measurements can be manipulated classically by randomization and post-processing [35–38]. We remark that the step of "Modulation" is designed to help us reduce the measurements from arbitrary forms to restricted ones, and this reduction heavily relies on the assumption (1), namely the independence of modulator and measurement device. Next, we prove that the restricted measurements $\{M_y\}$ is equivalent to the projective measurements $\{B_y\}$ proceeded by another channel, denoted by \mathcal{H} . In the view of security proof, we could pessimistically yield the channels \mathcal{G} and \mathcal{H} to Eve, namely \mathcal{G} and \mathcal{H} are absorbed to Eve's attack, which will never decrease her power. By doing so, we treat Bob's measurements as projective measurements in the security proof. In what follows, we will present a sketch of the security proof against collective attack.

First, we reduce the actual PM protocol to an EB version via successively introducing a series of virtual protocols, including the mirrored protocol, the symmetrized protocol, the renormalized protocol and finally the reduced EB protocol. In the mirrored protocol, we introduce Eve's collaborator, Fred, who controls the flaws in the devices, which follows the idea of the Gottesman-Lo-Lutkenhaus-Preiskill (GLLP) model [39], Fred applies a specific attack that provides Alice and Bob the same statistics, and Eve the same information gain. In the symmetrized protocol, we merge the mirrored protocol into the actual protocol. In the renormalized protocol, we renormalize the symmetrized protocol which means merging Eve's and Fred's attack together, and prove that such construction will provides Alice and Bob the same statistics, and Eve at least the same information gain as or maybe more than that of the actual protocol. In the reduced EB protocol, we remove the role of Fred, specify Eve's attack, and prove that it is equivalent to the renormalized protocol. Here we emphasize that introducing virtual protocols above can help us to let basis-dependent qubit source become basis-independent one, which is the key point of our proof. Second, based on the

first step, we prove that the shared two-qubit state ρ_{AB} in the reduced EB protocol has maximally mixed marginals. Therefore ρ_{AB} is equivalent to a Bell-diagonal state under local unitary transformation [40, 41], that is, one can choose an appropriate local reference frame so that ρ_{AB} is Bell-diagonal. And then we connect the amount of information leakage term to QD defined in Eq. (1), which actually has been proved in [18] by using Koashi-Winter relation [42], but we provide an alternative and easier proof for the Bell-diagonal state. Third, we consider the Bell-diagonal state in Bloch representation in Eq. (1) and prove Eq. (4), and finally obtain the key rate by using Devetak-Winter bound [43].

V. SIMULATION

Based on single photon source, we simulate the secure key rates against collective attack of DB-QKD and standard BB84 protocol under two specific quantum channels: depolarization channel and rotation channel. In the practical implementation, a depolarization channel is often resulted from the inevitable background error e.g. dark count on the detection side, a rotation channel is often resulted from the optical misalignment of imperfect optical components e.g. beam splitter or phase modulator. Therefore, depolarization channel and rotation channel are two typical channels and it is meaningful to discuss them.

By considering perfect BB84 state preparation and state measurement in our protocol, we derive the key rate under depolarization channel from Eq. (6). It's straightforward to see that $Q_{00} = Q_{11} = 1 - 2Q$ and $Q_{01} = Q_{10} = 0$ under depolarization channel, where Q is the quantum bit error rate (QBER) that quantifies the amount of depolarization. Then, we have $W = (1 - 2Q)^2$, and thus the key rate is $R \geq 1 - h(Q) - h(2Q - 2Q^2)$. For standard BB84 protocol, the key rate is $R \geq 1 - 2h(Q)$ [4]. In Fig. 1, in the case of depolarization channel, we find that DB-QKD can tolerate about 8% QBER, which is worse than the ones of standard BB84 protocol. It is straightforward to see that our method overestimates the information leakage so that the key rate is not as tight as the previous one.

By rotation channel, we mean a unitary rotation operation U on X - Z plane in Bloch sphere, that is, $U|0\rangle = \cos\theta/2|0\rangle - \sin\theta/2|1\rangle$ and $U|1\rangle = \sin\theta/2|0\rangle + \cos\theta/2|1\rangle$, where θ is the rotation angle. By considering perfect BB84 state preparation and state measurement in DB-QKD, we have $Q_{00} = Q_{11} = \cos\theta$ and $Q_{01} = -Q_{10} = \sin\theta$, and surprisingly find that the value $W = 1$ no matter what θ is. Moreover, the QBER is given by $Q = (1 - \cos\theta)/2$, and then the key rate is $R \geq 1 - h(Q)$ from Eq. (6). In Fig. 2, in the case of rotation channel, we find that DB-QKD can tolerate almost 50% QBER, which is much better than the ones of BB84 protocol. This is because we can put the dual of rotation operation to the measurement and equivalently view it as an

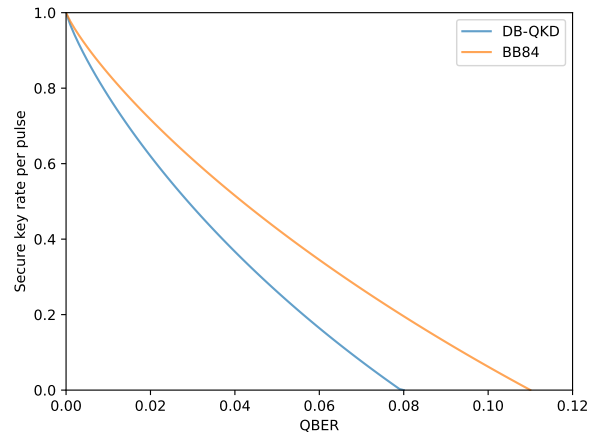


FIG. 1. Secure key rate versus QBER: The blue and the orange curve represent the secure key rates of DB-QKD and the standard BB84 protocol respectively, where a depolarization channel featured of QBER is considered. It shows that our protocol gives a lower key rate than the standard BB84 protocol for a depolarizing channel.

identity channel with measurements $\{U^\dagger B_y U\}$, and by making use of our proposed QD witness [21], then we tightly estimate the lower bound of $D(B|A)$. In other words, if considering rotation channel only, our method is able to tightly estimate the information leakage, which surpasses the previous methods. The above discussion is a specific example where perfect BB84 state preparation and state measurement are used, however, our method also applies to uncharacterized qubit preparation with a rotation channel in the certain Bloch plane, and similarly on qubit measurement side. This is because such witness construction of determinant is irrelative to the angle of such rotation, one can refer to Ref. [21] for more details.

VI. EXPERIMENT

Here we experimentally realize the DB-QKD in a phase encoding systems and demonstrate its advantages in imperfect preparation and measurement. We first conduct the protocol in the standard case to show the basic performance, where the states prepared are standard BB84 states and projectively measured without reference frame misalignment. Then the system, by contrast, runs in the cases of misalignment and uncharacterization, demonstrating the key-generation capability in imperfect scenarios. Especially, our protocol shows a much higher tolerance to reference frame rotation than standard BB84 protocol.

The experimental set-up is shown in Fig. 3. Alice acts as the transmitter, Bob is in charge of receiver, and they are linked by a 125 km optical fiber, corresponding to 22.5 dB of loss. The system adopts phase-encoding scheme and conducts three-intensity decoy-state protocol. The

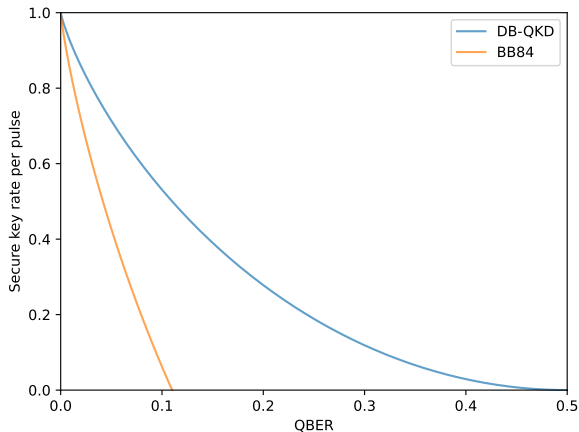


FIG. 2. Secure key rate versus QBER: The blue and the orange curve represent the secure key rates of DB-QKD and the standard BB84 protocol respectively, where a rotation channel featured of QBER is considered. It shows that our protocol gives a higher key rate than standard BB84 protocol for a rotation channel.

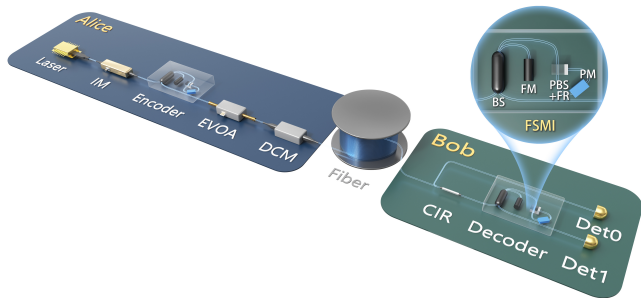


FIG. 3. Experimental schematic for the DB-QKD. Alice sends phase-encoding pulses to Bob via fiber. The misalignment and uncharacterization are caused by imperfect manipulation of encoder, decoder and channel. Laser, a gain-switched laser; IM, intensity modulator as the decoy-state modulator; Encoder and Decoder, conducting phase-encoding protocol which have the same structure of asymmetric Faraday-Sagnac-Michelson interferometer; EVOA, electronic variable optical attenuator; DCM, dispersion compensator module; Det, superconducting single photon detector.

qubits are encoded with basis \mathbb{Z} and \mathbb{X} , each basis has two orthogonal quantum states to carry binary information. The form of the four states is $\frac{1}{\sqrt{2}}(|s\rangle + e^{i\theta}|l\rangle)$, where the coded information is loaded by the phase difference, θ , of the two adjacent time-bin states, $|s\rangle$ and $|l\rangle$. In the standard case, $\theta \in \{0, \pi\}$ for \mathbb{Z} -basis and $\theta \in \{\frac{\pi}{2}, \frac{3\pi}{2}\}$ for \mathbb{X} -basis. The decoy-state protocol is used to estimate single-photon parameters using weak coherent states. Here we denote the three intensities as μ, ν, ω , they satisfy $\mu > \nu > \omega > 0$.

On Alice's side, the optical pulses are initially generated by a gain-switch laser, which is trigger by a 1.25 GHz clock signal. A dispersion compensator module (DCM) is used to counteract the pulse broadening caused by channel dispersion. The intensity modulator (IM) modulates the mean photon number of each pulse according to the decoy-state protocol and the electronic variable optical attenuator (EVOA) attenuates them to the single-photon level. The encoder is constructed by an asymmetric Faraday-Sagnac-Michelson interferometer (FSMI) [44], where a beamsplitter (BS) splits the laser pulse into two parts, one is reflected back by a Faraday Mirror within a short time, the other one travels along a Sagnac structure and its relative phase, θ_a , is randomly changed by the phase modulator (PM). The two parts corresponds to $|s\rangle$ and $|l\rangle$, respectively. The delay between them is set to 400 ps, a half of the period of 1.25 GHz.

On Bob's side, the decoder, with the same structure as Alice's encoder, decodes the pulses into two paths. Each path has a superconducting single photon detector (Det) to detect the pulse. The decoder of Bob decides the modulation and measurement basis. The random modulating phase, θ_B , of 0 and $\pi/2$ represents the standard projective measurements of \mathbb{Z} -basis and \mathbb{X} -basis, respectively. Bob also randomly adds a phase of 0 or π to θ_B to exchange the roles of Dets. Specifically, the added phase of 0 represents that the binary keys 0 and 1 are extracted from the clicks of Det0 and Det1, respectively. The added phase of π represents that the binary keys 0 and 1 are extracted from the clicks of Det1 and Det0, respectively. For double click events, the binary information is assigned randomly. The inter-pulse delay is also 400 ps, so the decoded pulse train is alternately arranged with interfering and non-interfering pulses. The insertion loss of receiver is 4.9 dB. Moreover, we filtrate the click event with a time window of 300 ps to reject irrelevant dark counts, only the events in the window are valid. The window width covers the whole pulses, whose full width at half maximum is about 130 ps including the optical pulse width and the timing jitter of click signals. So the dark count rates are lowered to 3×10^{-9} and 1.7×10^{-9} , respectively. The detection efficiency is 80%, whose mismatch between Det0 and Det1 is 1 : 1.25.

Then we demonstrate the DB-QKD protocol in three cases, those are standard, misaligned, and general cases, by choosing three specific examples. The experimental results are shown in Fig. 4. For the standard case, Alice prepares quantum states with $\theta_A \in \{0, \pi, \frac{\pi}{2}, \frac{3\pi}{2}\}$ and Bob projectively measures them by switching the θ_B between 0 and $\pi/2$, as well as randomly assigns the binary information. Due to the phase shift in devices and the channel, the phase reference should be compensated for a low error rate. For the misaligned case, the phase compensation is cancelled, we demonstrate the key distribution when the phase references of Alice and Bob are misaligned by $\pi/9$. This example reflects the effect of reference frame drift, which is the main challenge in practical

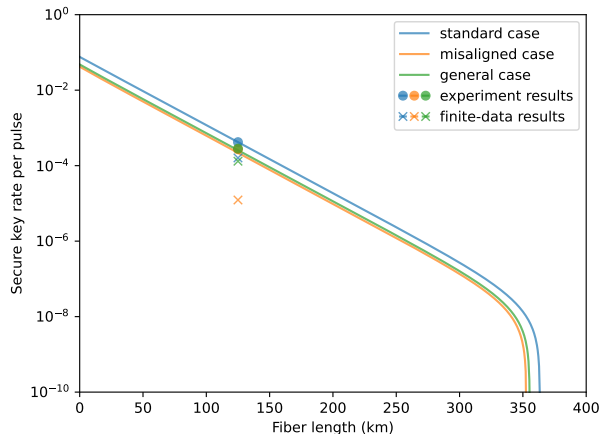


FIG. 4. Secret key rates of DB-QKD in the standard, misaligned, and general cases. The solid lines are simulation results. Experimental results are dotted around lines.

systems. For the general case, the quantum states prepared by Alice are mixed states, and the measurements conducted by Bob are POVMs. The general case demonstrates the secure key generation when both preparation and measurement are uncharacterized. Specifically, for each state, Alice prepares the standard states and misaligned states with equal probability resulting a mixed state of $\frac{1}{\sqrt{2}}(|s\rangle + e^{i\theta_A}|l\rangle)$ and $\frac{1}{\sqrt{2}}(|s\rangle + e^{i(\theta_A+\pi/9)}|l\rangle)$. Similarly, Bob modulates θ_b and $\theta_b + \pi/9$ with equal probability for each basis, as well as randomly assign the binary information, which forms POVMs. This example completely represents the imperfections of real devices, the result shows that our protocol can still distill secret key in this case, while the condition is beyond the security foundation of standard BB84 protocol. In each example, all system parameters are optimized for fair comparison. We finally obtain a secure key rate of 4.46×10^{-4} for the standard case. For the misaligned case and general case, the secret key rates are 2.45×10^{-4} and 2.17×10^{-4} , respectively. When the finite data effects are considered, the key rates slip to 2.45×10^{-4} , 1.02×10^{-5} , and 1.24×10^{-4} , respectively. Detailed data are listed in Supplementary Materials. The experimental results show that our protocol is capable to generate comparable key in general scenario while the standard BB84 protocol has been unadaptable. Although the uncharacterized preparation and measurement is beyond the security framework of standard BB84 protocol, they are still comparable in the misaligned case. So we further study the key-rate performance by rotating the phase reference between Alice and Bob. A surprising yet inevitable advantage of DB-QKD is revealed, our protocol can tolerate much higher misalignment than standard BB84 protocol.

The experimental results are shown in Fig. 5, where the solid blue line and dashed blue line respectively represent the simulated secret key rate of DB-QKD and stan-

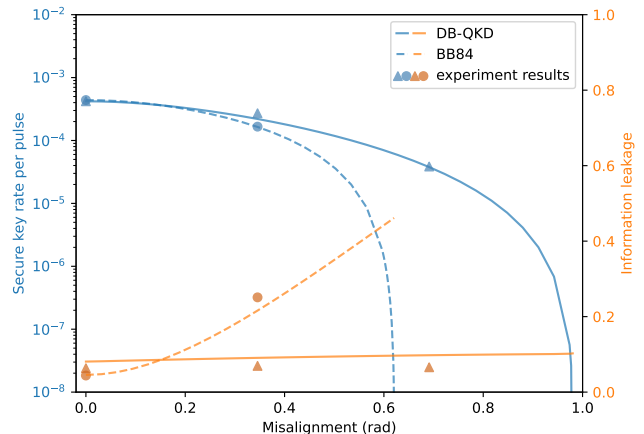


FIG. 5. Secret key rates of DB-QKD and BB84 as a function of misalignment degree. The solid and dashed lines are simulated key rates and information leakage, respectively. Experimental results are dotted around lines.

standard BB84 protocol with the channel of 125 km fiber. The blue dots and triangles are corresponding experimental results. The results shows a significant ability of DB-QKD on key generation in high misalignment scenario. The reason is the difference on estimating the information leakage. In standard BB84 protocol, we calculate the information leakage by single-photon phase error, $h(e_1)$, shown as the dashed orange line and dots in Fig. 5, while DB-QKD uses QD witness, $h(\frac{1-W}{2})$, shown as the solid orange line and triangles in Fig. 5. Phase error is sensitive to misalignment but QD witness is not, by using QD witness, the estimation of information leakage is tighter. The simulation of decoy DB-QKD can be found in Supplementary Materials.

VII. DISCUSSION AND CONCLUSION

In summary, we conclude our contributions in three aspects. At the fundamental level, we study the role of QD as a kind of quantum resource in our proposed protocol by showing the relation between QD and information leakage. Benefiting from our recently proposed QD witness [21], we successfully solve the long-standing problem of how to fully make use of discord to analyze security in quantum cryptography by linking the observable statistics to our QD witness [21]. At the technical level, we introduce new framework for security proof, which reduces the basis-dependent qubit source to a basis-independent one. At the practical level, our protocol in a manner that is immune to any imperfections of qubit-based processes, which is much more friendly to real-world implementation than the protocols demanding characterized quantum processes. Moreover, one can naturally lift the security against coherent attack using the existing meth-

ods, such as the postselection technique [45].

However, our theory still has its limitations, one of them being the dimension limitation. Taking standard decoy-state BB84 protocol as example, the imperfections beyond qubit pattern are not considered in DB-QKD, such as intensity fluctuation of light source [46–49], non-phase-randomized coherent state source [50–52] and so on [12]. Apart from the dimension limitation, an analysis of this scenario is established on the trusted devices. In other words, DB-QKD is not secure when the devices are malicious, such as blinding attack [53], Trojan-horse attacks [54] and other attacks caused by side channels [12]. We remark that, by combining measurement-device-independent (MDI) QKD [7] and the analysis of qubit preparation imperfection, some previous works [22–24] can achieve the goal of overcoming the imperfection of qubit pattern. But each of them demands stronger assumptions on qubit source, for example, it still need to

characterize qubit states in [22], pure qubit states are assumed in [23, 24]. Therefore, DB-QKD is different from previous works, and provides a new approach to tackle with imperfect devices.

ACKNOWLEDGMENTS

We cordially thank Hoi-Kwong Lo for many helpful discussions. R. W was supported by the University of Hong Kong start-up grant, G. -J. F. -Y, Z. -Q. Y, S. W, W. C, G. -C. G and Z. -F. H are supported by the National Natural Science Foundation of China (Grant Nos. 62105318, 62171424, 61961136004), the Fundamental Research Funds for the Central Universities, and the China Postdoctoral Science Foundation (2021M693098), H. -W. L is supported by NSAF (Grant no. U2130205), Y. Y is supported by National Natural Science Foundation of China (Grants No. 12175204).

SUPPLEMENTARY MATERIALS

In what follows we present the details that complement the main text. In section A, we reduce qubit measurements to projective measurements. In section B, we give the full security proof for our main result by information-theoretic approach and Devetak-Winter bound [43]. In section C, we take decoy-state into consideration and present the simulation method. Finally, in section D, we list the experimental data.

A. The reduction of qubit measurements

For each measurement $N \in \{N_y\}$, we now consider the form. Bob’s measurement can be assumed as two-outcome POVM within two-dimensional Hilbert space, and its general form is given by

$$N_c = \frac{[1 + (-1)^c K]I + (-1)^c \vec{T} \cdot \vec{\sigma}}{2}, \quad (7)$$

where $\{N_c\}$ denotes the elements of Bob’s POVMs, $\vec{\sigma} = (\sigma_x, \sigma_y, \sigma_z)$ is the Pauli matrix vector, \vec{T} is the Bloch vector, and K is a constant satisfying $0 \leq |K| \leq 1 - |\vec{T}|$. Here K is called the bias of the measurement, while $|\vec{T}|$ is called the sharpness [55, 56]. In fact, the step ”Modulation” in the actual protocol is designed to sharpen this bias. To see this, let’s take modulations $\{\mathcal{G}_z\}$ into consideration. If no such step ”Modulation”, the measurement outcomes are clearly $c \in \{0, 1\}$. With the step ”Modulation”, the measurement outcomes c are tagged by the modulation value $z \in \{0, 1\}$. By this tagging idea, we have a chance to re-assign the outcomes. Actually, we preserve the outcome if $z = 0$, flip it if $z = 1$, namely map c to $b \in \{0, 1\}$ by $b = c \oplus z$. Then, we use mathematical language to describe such classical process and see how this process sharpen the bias of the measurement. We can without loss of generality assume that the vector \vec{T} is in X - Z plane of Bloch sphere so that $-\vec{T} \cdot \vec{\sigma} = \sigma_y(\vec{T} \cdot \vec{\sigma})\sigma_y$. Note that we can assume this because there are only two measurement basis. Then, we have the following lemma.

Lemma 1. *Let*

$$M_b := \frac{I + (-1)^b \vec{T} \cdot \vec{\sigma}}{2}, \quad (8)$$

be the elements for measurement M . Let \mathcal{G} be a CPTP map such that $\mathcal{G}(\rho) = [\mathcal{G}_0(\rho) + \sigma_y \mathcal{G}_1(\rho) \sigma_y]/2$ for any incoming qubit ρ , then the difference of $\Pr[b = 0] - \Pr[b = 1]$ is given by

$$\Pr[b = 0] - \Pr[b = 1] = \text{Tr}[M_0 \mathcal{G}(\rho)] - \text{Tr}[M_1 \mathcal{G}(\rho)]. \quad (9)$$

Proof. For any incoming qubit ρ , the difference of $\Pr[b = 0] - \Pr[b = 1]$ is given by

$$\begin{aligned}
\Pr[b = 0] - \Pr[b = 1] &= \Pr[c \oplus z = 0] - \Pr[c \oplus z = 1] \\
&= \frac{1}{2} \text{Tr}[N_0 \mathcal{G}_0(\rho) + N_1 \mathcal{G}_1(\rho)] - \frac{1}{2} \text{Tr}[N_0 \mathcal{G}_1(\rho) + N_1 \mathcal{G}_0(\rho)] \\
&= \frac{1}{2} \text{Tr} \left[\frac{(1+K)I + \vec{T} \cdot \vec{\sigma}}{2} \mathcal{G}_0(\rho) + \frac{(1-K)I - \vec{T} \cdot \vec{\sigma}}{2} \mathcal{G}_1(\rho) \right] \\
&\quad - \frac{1}{2} \text{Tr} \left[\frac{(1-K)I + \vec{T} \cdot \vec{\sigma}}{2} \mathcal{G}_1(\rho) + \frac{(1+K)I - \vec{T} \cdot \vec{\sigma}}{2} \mathcal{G}_0(\rho) \right] \\
&= \text{Tr} \left[\frac{\vec{T} \cdot \vec{\sigma}}{2} \mathcal{G}_0(\rho) + \frac{\sigma_y (\vec{T} \cdot \vec{\sigma}) \sigma_y}{2} \mathcal{G}_1(\rho) \right] \\
&= \text{Tr} \left[\vec{T} \cdot \vec{\sigma} \frac{\mathcal{G}_0(\rho) + \sigma_y \mathcal{G}_1(\rho) \sigma_y}{2} \right] \\
&= \text{Tr}[M_0 \mathcal{G}(\rho)] - \text{Tr}[M_1 \mathcal{G}(\rho)],
\end{aligned} \tag{10}$$

where we insert Eq. (7) in the third equality, and make use of the assumption that $\{\mathcal{G}_z\}$ are CPTP maps, resulting in $\text{Tr}[\mathcal{G}_0(\rho) - \mathcal{G}_1(\rho)] = 0$, in the fourth equality. This complete our proof. \square

Clearly, this difference of probability is *independent* of the bias K . In this view, the process on Bob's side is reduced to *one* CPTP map \mathcal{G} followed by restricted measurements $\{M_y\}$, whose elements are given by

$$M_{b|y} := \frac{I + (-1)^b \vec{T}_y \cdot \vec{\sigma}}{2}. \tag{11}$$

In this way, we reduce the general two-outcome POVMs $\{N_y\}$ to the corresponding but restricted ones $\{M_y\}$. This reduction actually follows the idea that quantum measurements can be manipulated classically by randomization and post-processing [35–38].

Next, we prove that the POVMs $\{M_y\}$ can be decomposed as projective measurements $\{B_y\}$ proceeded by a CPTP map \mathcal{H} , as the following lemma shows.

Lemma 2. *Let*

$$B_{b|y} := \frac{I + (-1)^b \vec{B}_y \cdot \vec{\sigma}}{2}, \tag{12}$$

be the elements of each B_y , whose Bloch vectors \vec{B}_y are unit. Let $B_y := B_{0|y} - B_{1|y}$ and $M_y := M_{0|y} - M_{1|y}$, then there exists projective measurements $\{B_y\}$ and CPTP map \mathcal{H} such that $M_y = B_y \circ \mathcal{H}$.

Proof. Let $\{H_k\}$ be the Kraus operators for \mathcal{H} , then

$$\text{Tr}[B_y \mathcal{H}(\rho)] = \text{Tr} \left[B_y \sum_k H_k \rho H_k^\dagger \right] = \text{Tr} \left[\sum_k H_k^\dagger B_y H_k \rho \right], \tag{13}$$

for any incoming qubit ρ . As a consequence, it is equivalently to prove that

$$\mathcal{H}^\dagger(B_y) := \sum_k H_k^\dagger B_y H_k = M_y. \tag{14}$$

For the simplicity of proof, we shall choose a specific reference frame. Without loss of generality, let $M_0 = s_{0z} \sigma_z$ and $M_1 = s_{1x} \sigma_x + s_{1z} \sigma_z$ where \vec{s}_0 and \vec{s}_1 are in X - Z plane of Bloch sphere, and $|\vec{s}_0| \geq |\vec{s}_1|$, we find \mathcal{H}_1 that

$$\mathcal{H}_1(\sigma_z) = \frac{1 + s_{0z}}{2} I \sigma_z I + \frac{1 - s_{0z}}{2} \sigma_y \sigma_z \sigma_y = M_0, \tag{15}$$

simultaneously, we have

$$\mathcal{H}_1\left(\frac{s_{1x} \sigma_x + s_{1z} \sigma_z}{s_{0z}}\right) = M_1. \tag{16}$$

Next, we find \mathcal{H}_2 that

$$\mathcal{H}_2(\sigma_z) = \frac{1}{2}\left(1 + \frac{s_{1x}}{\sqrt{s_{0z}^2 - s_{1z}^2}}\right)I\sigma_z I + \frac{1}{2}\left(1 - \frac{s_{1x}}{\sqrt{s_{0z}^2 - s_{1z}^2}}\right)\sigma_z\sigma_z\sigma_z = \sigma_z, \quad (17)$$

if $s_{0z} \neq s_{1z}$, and set \mathcal{H}_2 as the identity channel if $s_{0z} = s_{1z}$. Simultaneously, we have

$$\mathcal{H}_2\left(\frac{\sqrt{s_{0z}^2 - s_{1z}^2}\sigma_x + s_{1z}\sigma_z}{s_{0z}}\right) = \frac{s_{1x}\sigma_x + s_{1z}\sigma_z}{s_{0z}}, \quad (18)$$

finally, we set $B_0 = \sigma_z$, $B_1 = (\sqrt{s_{0z}^2 - s_{1z}^2}\sigma_x + s_{1z}\sigma_z)/s_{0z}$ and $\mathcal{H}^\dagger = \mathcal{H}_1 \circ \mathcal{H}_2$, which completes the proof. \square

Finally, we pessimistically yield the CPTP maps \mathcal{G} and \mathcal{H} to Eve, namely \mathcal{G} and \mathcal{H} are absorbed to Eve's attack, which will never decrease Eve's information gain. And we remove the step of "Modulation" and treat Bob's measurements as $\{B_y\}$ in the following.

B. Full security proof of DB-QKD protocol

Step 1: Constructing the Reduced Entanglement-Based Protocol.

As said in the main text, the first step for security proof is to construct a reduced EB version of the actual protocol by successively introducing a series of virtual protocols, including the mirrored protocol, the symmetrized protocol, the renormalized protocol and finally the reduced EB protocol. Thus, we start from the actual protocol. The brief picture of the actual protocol is shown in Fig. 6, where $\{\tau_{x,a}\}$ of system B are Alice's emitting qubits, \mathcal{E} is the completely positive trace non-increasing map describing Eve's attack, $\tau_{x,a}^e := \mathcal{E}(\tau_{x,a})/\text{Tr}[\mathcal{E}(\tau_{x,a})]$ are Bob's receiving qubits, respectively, $\{B_y\}$ are Bob's measurements.

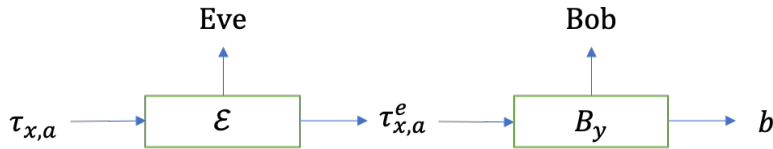


FIG. 6. The brief picture of the actual protocol.

Now, we introduce the mirrored protocol, the brief picture is shown in Fig. 7. In the mirrored protocol, Fred locates in Alice's device, prepares corresponding qubit $\bar{\tau}_{x,a} := I - \tau_{x,a} \otimes 1$ of system B for each (x, a) , applies a specific channel $\bar{\mathcal{E}}$ that $\bar{\tau}_{x,a}^e := \bar{\mathcal{E}}(\bar{\tau}_{x,a})/\text{Tr}[\bar{\mathcal{E}}(\bar{\tau}_{x,a})]$, respectively. Then, Fred is permitted to send $\{\bar{\tau}_{x,a}\}$ to Bob for measurements $\{B_y\}$ and ancillary system to Eve for further processing, respectively. The details of the mirrored protocol are showed in Tab. II. In terms of the emitted qubits, figuratively speaking, for each basis x , the Bloch vector corresponding to $\{\tau_{x,0}\}$ and the Bloch vector corresponding to $\{\bar{\tau}_{x,1}\}$ are opposite vectors, the schematic diagram can be found in Fig. 8.

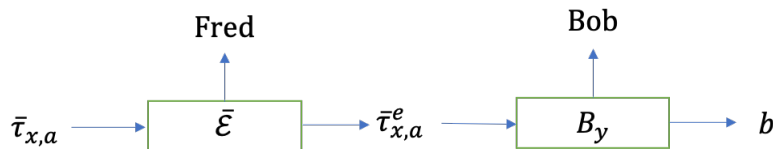


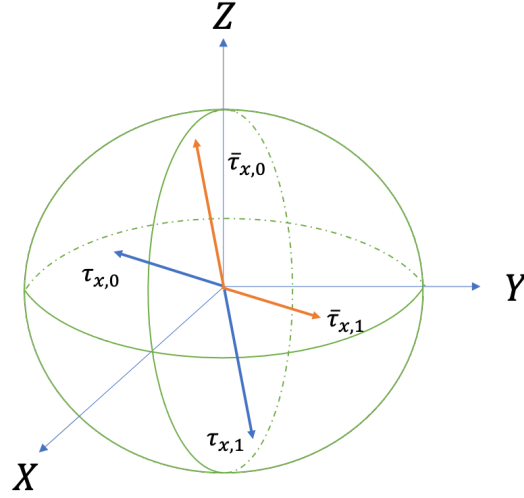
FIG. 7. The brief picture of the mirrored protocol.

To prove that the mirrored protocol provides the same statistics and information leakage as that of the actual protocol, we refer to Choi–Jamiolkowski isomorphism (also called channel-state duality somewhere) to describe the quantum channel. Suppose we introduce a two-dimensional system denoted as A , in the actual protocol, Alice sends a qubit state of system B to Bob through channel \mathcal{E} , then \mathcal{E} can completely specified by the non-normalized state

$$\sigma_{AB} := (\mathcal{I}_A \otimes \mathcal{E})P\{|00\rangle_{AB} + |11\rangle_{AB}\}, \quad (19)$$

TABLE II. The mirrored protocol

-
- **State preparation:** In each round, Alice randomly chooses a preparation basis $x \in \{0, 1\}$. Next, Alice chooses a uniformly random bit value $a \in \{0, 1\}$ as her raw data. Fred knows (x, a) .
 - **Distribution:** In each round, Fred manipulates the source device to send $\bar{\tau}_{x,a}$ to Bob through the insecure channel $\bar{\mathcal{E}}$.
 - **Measurement:** In each round, Bob randomly chooses a measurement basis $y \in \{0, 1\}$, measurement device performs the projective measurements B_y , and then, outputs a bit value $b \in \{0, 1\}$ as Bob's raw data.
 - **Collaboration:** In each round, Fred sends the ancillary system E to Eve.
 - **Parameter estimation:** Alice and Bob publicly announce a part of their raw data and calculate the bit error for each basis combination (x, y) . If the secret key rate calculated from these distributions is positive, then continue the protocol, if not, abort the protocol.
 - **Key generation:** Alice and Bob keep the leftover data of $x = y = 0$ for the final secure key extraction.
 - **Post-processing:** Alice and Bob perform a direct information reconciliation including error correction and privacy amplification to obtain the final secret key.
-

FIG. 8. The geometric relations between $\tau_{x,a}$ and $\bar{\tau}_{x,a \oplus 1}$ for each basis x .

where \mathcal{I}_A is the identity map on system A , $P\{|\cdot\rangle\} := |\cdot\rangle\langle\cdot|$ represents a pure state, and $|00\rangle_{AB} + |11\rangle_{AB}$ is, up to a normalization factor, a maximally entangled state of the systems A and B . Then, for any Alice's emitting qubit state $\tau \in \{\tau_{x,a}\}$ of system B , Bob's sub-normalized receiving qubit is given by

$$\mathcal{E}(\tau) = \text{Tr}_A[\tau^* \sigma_{AB}], \quad (20)$$

where τ^* of system A is the complex conjugate of τ , and thus the corresponding transmission rate is $\text{Tr}[\mathcal{E}(\tau)]$. In the actual protocol, let

$$\sigma_{AB} = \sum_{j=1}^4 |s_j\rangle\langle s_j| = \sum_{j=1}^4 P\{\sqrt{\alpha_j} |\alpha_j\rangle_A |\alpha_j\rangle_B + \sqrt{\beta_j} |\beta_j\rangle_A |\beta_j\rangle_B\}, \quad (21)$$

be the spectrum decomposition of σ_{AB} , where α_j and β_j are some non-negative and real coefficients for each j , $|\alpha_j\rangle$ and $|\beta_j\rangle$ are mutually orthogonal states for each j , so that $|s_j\rangle := \sqrt{\alpha_j} |\alpha_j\rangle_A |\alpha_j\rangle_B + \sqrt{\beta_j} |\beta_j\rangle_A |\beta_j\rangle_B$ is written in the form of Schmidt decomposition for each j . In the mirrored protocol, we specify $\bar{\mathcal{E}}$ as

$$\bar{\sigma}_{AB} := (\mathcal{I}_A \otimes \bar{\mathcal{E}})P\{|00\rangle_{AB} + |11\rangle_{AB}\} = \sum_{j=1}^4 |\bar{s}_j\rangle\langle \bar{s}_j| = \sum_{j=1}^4 P\{\sqrt{\alpha_j} |\beta_j\rangle_A |\beta_j\rangle_B + \sqrt{\beta_j} |\alpha_j\rangle_A |\alpha_j\rangle_B\} \quad (22)$$

where $|\bar{s}_j\rangle := \sqrt{\alpha_j} |\beta_j\rangle_A |\beta_j\rangle_B + \sqrt{\beta_j} |\alpha_j\rangle_A |\alpha_j\rangle_B$. Now, we are ready to prove that $\bar{\mathcal{E}}$ provides Alice and Bob the same statistics.

Lemma 3. *In the mirrored protocol, Fred will provide Alice and Bob the same Q and W as that of the actual protocol.*

Proof. First, we show that $\bar{\sigma}_{AB}^* = (\sigma_y \otimes \sigma_y) \sigma_{AB} (\sigma_y \otimes \sigma_y)$, where $\bar{\sigma}_{AB}^*$ is the complex conjugate of $\bar{\sigma}_{AB}$. For any two mutually orthogonal states $|\alpha\rangle_A \in \{|\alpha_j\rangle_A\}$ and $|\beta\rangle_A \in \{|\beta_j\rangle_A\}$, they can be expressed by

$$\begin{aligned} |\alpha\rangle_A &= \cos \theta_A |0\rangle + e^{i\phi_A} \sin \theta_A |1\rangle \\ |\beta\rangle_A &= e^{i\gamma_A} (\sin \theta_A |0\rangle - e^{i\phi_A} \cos \theta_A |1\rangle), \end{aligned} \quad (23)$$

up to a global phase, where θ_A , ϕ_A and γ_A are some real numbers then we see that

$$\begin{aligned} \sigma_y |\alpha\rangle_A &= e^{i(\phi_A + \gamma_A - \frac{\pi}{2})} |\beta^*\rangle_A \\ \sigma_y |\beta\rangle_A &= e^{i(\phi_A + \gamma_A + \frac{\pi}{2})} |\alpha^*\rangle_A, \end{aligned} \quad (24)$$

where $|\alpha^*\rangle_A$ and $|\beta^*\rangle_A$ are the complex conjugate of $|\alpha\rangle_A$ and $|\beta\rangle_A$, respectively, thus we have

$$\begin{aligned} (\sigma_y \otimes \sigma_y) |\alpha\rangle_A |\alpha\rangle_B &= e^{i(\phi_A + \gamma_A + \phi_B + \gamma_B - \pi)} |\beta^*\rangle_A |\beta^*\rangle_B \\ (\sigma_y \otimes \sigma_y) |\beta\rangle_A |\beta\rangle_B &= e^{i(\phi_A + \gamma_A + \phi_B + \gamma_B + \pi)} |\alpha^*\rangle_A |\alpha^*\rangle_B, \end{aligned} \quad (25)$$

where ϕ_B and γ_B are some real numbers, $|\alpha\rangle_B \in \{|\alpha_j\rangle_B\}$ and $|\beta\rangle_B \in \{|\beta_j\rangle_B\}$ are mutually orthogonal states, and $|\alpha^*\rangle_B$ and $|\beta^*\rangle_B$ are their complex conjugate, respectively. As a consequence, for any $|s\rangle \in \{|s_j\rangle\}$ and $|\bar{s}\rangle \in \{|\bar{s}_j\rangle\}$, we have

$$(\sigma_y \otimes \sigma_y) |s\rangle = e^{i\omega} |\bar{s}^*\rangle, \quad (26)$$

where $|\bar{s}^*\rangle$ is the complex conjugate of $|\bar{s}\rangle$, $\omega = \phi_A + \gamma_A + \phi_B + \gamma_B + \pi$. Therefore, for each j , $|s_j\rangle$ differs from $|\bar{s}_j\rangle$ by a local unitary transportation $\sigma_y \otimes \sigma_y$ followed by replacement with complex conjugate (i.e. operation of transpose), that is

$$\sigma_y \otimes \sigma_y |s_j\rangle = e^{i\omega_j} |\bar{s}_j^*\rangle, \quad (27)$$

where ω_j is a global phase, $|\bar{s}_j^*\rangle$ is the complex conjugate of $|\bar{s}_j\rangle$, which completes the first part of proof.

Second, to calculate the observable statistics, for each (x, a) , we consider the transmission rate $Y_{x,a} := \text{Tr}[\mathcal{E}(\tau_{x,a})]$ in the actual protocol and $\bar{Y}_{x,a} := \text{Tr}[\bar{\mathcal{E}}(\bar{\tau}_{x,a})]$ in the mirrored protocol, and show that $Y_{x,a} = \bar{Y}_{x,a \oplus 1}$. For each (x, a) , we define

$$\begin{aligned} \tau_{x,a} &:= \mu_{x,a} |\mu_{x,a}\rangle \langle \mu_{x,a}| + \nu_{x,a} |\nu_{x,a}\rangle \langle \nu_{x,a}| \\ \bar{\tau}_{x,a} &= I - \tau_{x,a} := \nu_{x,a} |\mu_{x,a}\rangle \langle \mu_{x,a}| + \mu_{x,a} |\nu_{x,a}\rangle \langle \nu_{x,a}|, \end{aligned} \quad (28)$$

as the spectrum decomposition of $\tau_{x,a}$ and $\bar{\tau}_{x,a}$, respectively, where $\mu_{x,a}$ and $\nu_{x,a}$ are real coefficients satisfying $0 \leq \nu_{x,a} \leq \mu_{x,a} \leq 1$ and $\mu_{x,a} + \nu_{x,a} = 1$, $|\mu_{x,a}\rangle$ and $|\nu_{x,a}\rangle$ are mutually orthogonal states, then we write the complex conjugate of $\tau_{x,a}$ as $\tau_{x,a}^* := \mu_{x,a} |\mu_{x,a}^*\rangle \langle \mu_{x,a}^*| + \nu_{x,a} |\nu_{x,a}^*\rangle \langle \nu_{x,a}^*|$, the complex conjugate of $\bar{\tau}_{x,a}$ as $\bar{\tau}_{x,a}^* := \nu_{x,a} |\mu_{x,a}^*\rangle \langle \mu_{x,a}^*| + \mu_{x,a} |\nu_{x,a}^*\rangle \langle \nu_{x,a}^*|$, where $|\mu_{x,a}^*\rangle$ and $|\nu_{x,a}^*\rangle$ are the complex conjugate of $|\mu_{x,a}\rangle$ and $|\nu_{x,a}\rangle$, respectively. Then, for any pure state $|\mu^*\rangle \in \{|\mu_{x,a}^*\rangle\}$ and $|\nu^*\rangle \in \{|\nu_{x,a}^*\rangle\}$, and any state $|s\rangle \in \{|s_j\rangle\}$ and $|\bar{s}\rangle \in \{|\bar{s}_j\rangle\}$, we have

$$\text{Tr}[|\mu^*\rangle \langle \mu^*| s\rangle \langle s|] = \alpha |\langle \mu^* | \alpha \rangle_A|^2 + \beta |\langle \nu^* | \alpha \rangle_A|^2 = \alpha |\langle \nu^* | \beta \rangle_A|^2 + \beta |\langle \mu^* | \beta \rangle_A|^2 = \text{Tr}[|\nu^*\rangle \langle \nu^*| \bar{s}\rangle \langle \bar{s}|]. \quad (29)$$

where we make use of the fact that $|\langle \mu^* | \alpha \rangle_A| = |\langle \nu^* | \beta \rangle_A|$ and $|\langle \nu^* | \alpha \rangle_A| = |\langle \mu^* | \beta \rangle_A|$. As a consequence, inserting Eq. (20), Eq. (21) and Eq. (22), we derive that

$$\begin{aligned} Y_{x,a} &= \text{Tr}[\mathcal{E}(\tau_{x,a})] \\ &= \text{Tr}[\tau_{x,a}^* \sigma_{AB}] \\ &= \sum_{j=1}^4 \text{Tr}[(\mu_{x,a} |\mu_{x,a}^*\rangle \langle \mu_{x,a}^*| + \nu_{x,a} |\nu_{x,a}^*\rangle \langle \nu_{x,a}^*|) |s_j\rangle \langle s_j|] \\ &= \sum_{j=1}^4 \text{Tr}[(\mu_{x,a} |\nu_{x,a}^*\rangle \langle \nu_{x,a}^*| + \nu_{x,a} |\mu_{x,a}^*\rangle \langle \mu_{x,a}^*|) |\bar{s}_j\rangle \langle \bar{s}_j|] \\ &= \text{Tr}[\bar{\tau}_{x,a \oplus 1}^* \bar{\sigma}_{AB}] \\ &= \text{Tr}[\bar{\mathcal{E}}(\bar{\tau}_{x,a \oplus 1})] \\ &= \bar{Y}_{x,a \oplus 1}, \end{aligned} \quad (30)$$

for each (x, a) , which completes the second part of proof.

Third, for each (x, a) , we show that $\tau_{x,a}^e + \bar{\tau}_{x,a\oplus 1}^e = I$. Similarly, for any pure state $|\mu^*\rangle \in \{|\mu_{x,a}^*\rangle\}$ and $|\nu^*\rangle \in \{|\nu_{x,a}^*\rangle\}$, and any state $|s\rangle \in \{|s_j\rangle\}$ and $|\bar{s}\rangle \in \{|\bar{s}_j\rangle\}$, we have

$$\begin{aligned} & \text{Tr}_A[|\mu^*\rangle \langle \mu^*|s\rangle \langle s|] + \text{Tr}_A[|\nu^*\rangle \langle \nu^*|\bar{s}\rangle \langle \bar{s}|] \\ &= P\{\sqrt{\alpha} \langle \mu^*|\alpha\rangle_A |\alpha\rangle_B + \sqrt{\beta} \langle \mu^*|\beta\rangle_A |\beta\rangle_B\} + P\{\sqrt{\alpha} \langle \nu^*|\beta\rangle_A |\beta\rangle_B + \sqrt{\beta} \langle \nu^*|\alpha\rangle_A |\alpha\rangle_B\} \\ &= (\alpha |\langle \mu^*|\alpha\rangle_A|^2 + \beta |\langle \nu^*|\alpha\rangle_A|^2) |\alpha\rangle_B \langle \alpha| + (\alpha |\langle \nu^*|\beta\rangle_A|^2 + \beta |\langle \mu^*|\beta\rangle_A|^2) |\beta\rangle_B \langle \beta| \\ &\propto I, \end{aligned} \quad (31)$$

where we make use of the facts that $|\langle \mu^*|\alpha\rangle_A| = |\langle \nu^*|\beta\rangle_A|$ and $|\langle \nu^*|\alpha\rangle_A| = |\langle \mu^*|\beta\rangle_A|$ again so that the two diagonal terms are same, and the fact that $\langle \mu^*|\alpha\rangle_A \langle \beta|\mu^*\rangle + \langle \nu^*|\alpha\rangle_A \langle \beta|\nu^*\rangle = \text{Tr}[\alpha]_A \langle \beta| = 0$ and $\langle \mu^*|\beta\rangle_A \langle \alpha|\mu^*\rangle + \langle \nu^*|\beta\rangle_A \langle \alpha|\nu^*\rangle = \text{Tr}[\beta]_A \langle \alpha| = 0$ so that the two non-diagonal terms vanish. By swapping $|\mu^*\rangle$ and $|\nu^*\rangle$, we have

$$\text{Tr}_A[|\nu^*\rangle \langle \nu^*|s\rangle \langle s|] + \text{Tr}_A[|\mu^*\rangle \langle \mu^*|\bar{s}\rangle \langle \bar{s}|] \propto I. \quad (32)$$

Inserting Eq. (31), Eq. (32) and $Y_{x,a} = \bar{Y}_{x,a\oplus 1}$, we have

$$\begin{aligned} \tau_{x,a}^e + \bar{\tau}_{x,a\oplus 1}^e &= \frac{\mathcal{E}(\tau_{x,a})}{\text{Tr}[\mathcal{E}(\tau_{x,a})]} + \frac{\bar{\mathcal{E}}(\bar{\tau}_{x,a\oplus 1})}{\text{Tr}[\bar{\mathcal{E}}(\bar{\tau}_{x,a\oplus 1})]} \\ &= \frac{1}{Y_{x,a}} \sum_{j=1}^4 \text{Tr}_A[(\mu_{x,a} |\mu_{x,a}^*\rangle \langle \mu_{x,a}^*| + \nu_{x,a} |\nu_{x,a}^*\rangle \langle \nu_{x,a}^*|) |s_j\rangle \langle s_j|] \\ &\quad + \frac{1}{\bar{Y}_{x,a\oplus 1}} \sum_{j=1}^4 \text{Tr}_A[(\mu_{x,a} |\nu_{x,a}^*\rangle \langle \nu_{x,a}^*| + \nu_{x,a} |\mu_{x,a}^*\rangle \langle \mu_{x,a}^*|) |\bar{s}_j\rangle \langle \bar{s}_j|] \\ &= \frac{1}{Y_{x,a}} \sum_{j=1}^4 \mu_{x,a} (\text{Tr}_A[|\mu_{x,a}^*\rangle \langle \mu_{x,a}^*|s_j\rangle \langle s_j|] + \text{Tr}_A[|\nu_{x,a}^*\rangle \langle \nu_{x,a}^*|\bar{s}_j\rangle \langle \bar{s}_j|]) \\ &\quad + \frac{1}{Y_{x,a}} \sum_{j=1}^4 \nu_{x,a} (\text{Tr}_A[|\nu_{x,a}^*\rangle \langle \nu_{x,a}^*|s_j\rangle \langle s_j|] + \text{Tr}_A[|\mu_{x,a}^*\rangle \langle \mu_{x,a}^*|\bar{s}_j\rangle \langle \bar{s}_j|]) \\ &\propto I, \end{aligned} \quad (33)$$

and due to the fact that $\text{Tr}[\tau_{x,a}^e] + \text{Tr}[\bar{\tau}_{x,a\oplus 1}^e] = 2$, we see that $\tau_{x,a}^e + \bar{\tau}_{x,a\oplus 1}^e = I$, which completes the third part of proof.

Finally, we come to the proof regarding to the statistics. As the definition in the main text, Q and W are determined by the bit error e_{xy} of each (x, y) , in the actual protocol, to calculate the bit error, we define the count rate as

$$G_{a,b|x,y} := Y_{x,a} \text{Tr}[\tau_{x,a}^e B_{b|y}], \quad (34)$$

for each (a, b) conditioned on (x, y) , therefore,

$$e_{xy} := \frac{\sum_{a \neq b} G_{a,b|x,y}}{\sum_{a,b} G_{a,b|x,y}}. \quad (35)$$

Similarly, the bit error for each (x, y) in the mirrored protocol is given by

$$\bar{e}_{xy} := \frac{\sum_{a \neq b} \bar{G}_{a,b|x,y}}{\sum_{a,b} \bar{G}_{a,b|x,y}}. \quad (36)$$

where

$$\bar{G}_{a,b|x,y} := \bar{Y}_{x,a} \text{Tr}[\bar{\tau}_{x,a}^e M_{b|y}]. \quad (37)$$

By Eq. (11) and $\tau_{x,a}^e + \bar{\tau}_{x,a\oplus 1}^e = I$, we have

$$\text{Tr}[\tau_{x,a}^e B_{b|y}] = \text{Tr}[\bar{\tau}_{x,a\oplus 1}^e B_{b\oplus 1|y}], \quad (38)$$

and immediately obtain

$$G_{a,b|x,y} = Y_{x,a} \text{Tr}[\tau_{x,a}^e B_{b|y}] = \bar{Y}_{x,a\oplus 1} \text{Tr}[\bar{\tau}_{x,a\oplus 1}^e B_{b\oplus 1|y}] = \bar{G}_{a\oplus 1,b\oplus 1|x,y}, \quad (39)$$

where we make use of the facts that $Y_{x,a} = \bar{Y}_{x,a\oplus 1}$, and thus $e_{xy} = \bar{e}_{xy}$, which completes the proof. \square

In order to evaluate Eve's information gain, we refer to the Stinespring dilation picture that describes a quantum channel as unitary transformation followed by a partial trace. Let $U_{\mathcal{E}}$ on the system B and Eve's ancillary system E be the corresponding unitary transformation of \mathcal{E} , then Eve's attack can be specified by the non-normalized tripartite state

$$|\Phi\rangle_{ABE} := |\text{filter}\rangle \langle \text{filter}| U_{\mathcal{E}}(|00\rangle_{AB} + |11\rangle_{AB}) |e\rangle_E = \sum_{j=1}^4 |s_j\rangle |e_j\rangle_E, \quad (40)$$

where $|\text{filter}\rangle \langle \text{filter}|$ on system B corresponds to a non-demolition measurement that determines whether an efficient detection occurs, $|e\rangle_E$ is Eve's initial ancilla, the normalized states $|e_j\rangle_E$ of system E are mutually orthogonal, so that $|\Phi\rangle_{ABE}$ is also written in the form of Schmidt decomposition. Considering Eq. (21), we can map $|\Phi\rangle_{ABE}$ to σ_{AB} by partially tracing system E out, that is, $\sigma_{AB} = \text{Tr}[|\Phi\rangle_{ABE} \langle \Phi|]$, thus $|\Phi\rangle_{ABE}$ can completely describe the quantum channel \mathcal{E} and help evaluate Eve's information gain. Similarly, in the mirrored protocol, let $U_{\bar{\mathcal{E}}}$ on the system B and system E be the corresponding unitary transformation of $\bar{\mathcal{E}}$, then Fred's limited attack can be specified by the non-normalized tripartite state

$$|\bar{\Phi}\rangle_{ABE} := |\text{filter}\rangle \langle \text{filter}| U_{\bar{\mathcal{E}}}(|00\rangle_{AB} + |11\rangle_{AB}) |e\rangle_E = \sum_{j=1}^4 |\bar{s}_j\rangle |e_j\rangle_E. \quad (41)$$

Now, we are ready to prove that $\bar{\mathcal{E}}$ provides Eve the same information gain.

Lemma 4. *In the mirrored protocol, Fred will provide Eve the same information knowledge as that of the actual protocol.*

Proof. In the actual protocol, if considering the key generation basis $x = y = 0$ only, the state after implementing B_0 is given by

$$\rho_{ABE} = \sum_{a,b} |ab\rangle_{AB} \langle ab| \otimes \rho_{E|a,b}, \quad (42)$$

where,

$$\rho_{E|a,b} = \text{Tr}_{AB}[(\tau_{0,a}^* \otimes B_{b|0}) |\Phi\rangle_{ABE} \langle \Phi|] = \text{Tr}_{AB}[(\tau_{0,a}^* \otimes M_{b|0}) P\{\sum_{j=1}^4 |s_j\rangle |e_j\rangle_E\}], \quad (43)$$

and Eve's information gain is determined by ρ_{ABE} . Concretely, Eve's information gain is determined by the uncertainty of classical bit a conditioned on her system E , which is featured by the conditional entropy $H(A|E)$. By standard calculation, $H(A|E)$ is determined by the eigenvalues of states $\text{Tr}_B[\rho_{ABE}]$ and $\text{Tr}_{AB}[\rho_{ABE}]$, respectively. Similarly, in the mirrored protocol, we have state as

$$\bar{\rho}_{ABE} = \sum_{a,b} |ab\rangle_{AB} \langle ab| \otimes \bar{\rho}_{E|a,b}, \quad (44)$$

where

$$\bar{\rho}_{E|a,b} = \text{Tr}_{AB}[(\bar{\tau}_{0,a}^* \otimes M_{b|0}) |\bar{\Phi}\rangle_{ABE} \langle \bar{\Phi}|] = \text{Tr}_{AB}[(\bar{\tau}_{0,a}^* \otimes B_{b|0}) P\{\sum_{j=1}^4 |\bar{s}_j\rangle |e_j\rangle_E\}]. \quad (45)$$

For the simplicity of proof, we choose a specific reference frame that the corresponding Bloch vectors of $\{\tau_{0,a}\}$ and $\{B_{b|0}\}$ lie in the X - Z plane of Bloch sphere, then we have $\sigma_y \tau_{0,a}^* \sigma_y = \bar{\tau}_{0,a \oplus 1}^*$ and $\sigma_y B_{b|0} \sigma_y = B_{b \oplus 1|0}$. Inserting Eq. (27), we have

$$\begin{aligned} \text{Tr}_{AB}[(\tau_{0,a}^* \otimes B_{b|0}) P\{\sum_{j=1}^4 |s_j\rangle |e_j\rangle_E\}] &= \text{Tr}_{AB}[(\sigma_y \tau_{0,a}^* \sigma_y \otimes \sigma_y B_{b|0} \sigma_y) P\{\sigma_y \otimes \sigma_y \sum_{j=1}^4 |s_j\rangle |e_j\rangle_E\}] \\ &= \text{Tr}_{AB}[(\bar{\tau}_{0,a \oplus 1}^* \otimes B_{b \oplus 1|0}) P\{\sum_{j=1}^4 e^{i\omega_j} |\bar{s}_j^*\rangle |e_j\rangle_E\}] \\ &= \text{Tr}_{AB}[(\bar{\tau}_{0,a \oplus 1}^* \otimes B_{b \oplus 1|0}) P\{U_{\text{ph}} \sum_{j=1}^4 |\bar{s}_j^*\rangle |e_j\rangle_E\}], \end{aligned} \quad (46)$$

where $U_{\text{ph}} = \sum_{j=1}^4 e^{i\omega_j} |e_j\rangle_E \langle e_j|$ is a unitary transformation on system E . Due to Eq. (43) and Eq. (45), we have

$$\rho_{E|a,b} = U_{\text{ph}} \bar{\rho}_{E|a\oplus 1, b\oplus 1}^* U_{\text{ph}}^\dagger, \quad (47)$$

where $\bar{\rho}_{E|a\oplus 1, b\oplus 1}^*$ is the complex conjugate of $\bar{\rho}_{E|a\oplus 1, b\oplus 1}$, so that $\bar{\rho}_{ABE}$ differs from ρ_{ABE} by a common bit flipping operation on systems A and B and a unitary transformation on system E , followed by the replacement with complex conjugate. These operations result in the same eigenvectors of $\text{Tr}_B[\rho_{ABE}]$ and $\text{Tr}_B[\bar{\rho}_{ABE}]$, as well as that of $\text{Tr}_{AB}[\rho_{ABE}]$ and $\text{Tr}_{AB}[\bar{\rho}_{ABE}]$, thus Eve's information gain is totally same in the actual and mirrored protocols, which completes the proof. \square

Next, we merge the mirrored protocol into the actual protocol, and introduce a symmetrized protocol, the brief picture is shown in Fig. 9. In this symmetrized protocol, Fred also knows the all information on Alice's side, moreover, he is permitted to uniformly at random choose a state $|g_0\rangle$ or $|g_1\rangle$ of system G , if $|g_0\rangle$ chosen, the actual protocol will be executed, if $|g_1\rangle$ chosen, the mirrored protocol will be executed, before the public discussion between Alice and Bob, Fred sends ancillary system as well as the system G to Eve. The details of the symmetrized are showed in Tab. III. From the perspective of Alice and Bob, the emitted states are actually $\rho_{x,a} := (\tau_{x,a} + \bar{\tau}_{x,a})/2$ in the symmetrized protocol. In Fig. 10, we show the geometric relationship between $\{\tau_{x,a}\}$, $\{\bar{\tau}_{x,a}\}$ and $\{\rho_{x,a}\}$, it is easy to verify that, in the symmetrized protocol, the basis-dependent states that of $\tau_{0,0} + \tau_{0,1} \neq \tau_{1,0} + \tau_{1,1}$ become basis-independent that of $\rho_{0,0} + \rho_{0,1} = \rho_{1,0} + \rho_{1,1} = I$. Based on Lemma 3 and Lemma 4, we obtain the following corollary.

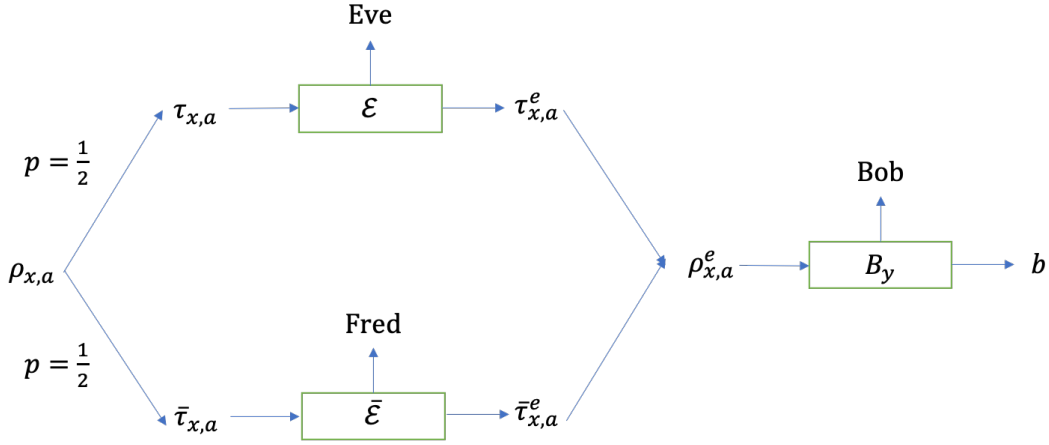


FIG. 9. The brief picture of the symmetrized protocol.

TABLE III. The symmetrized protocol

-
- **State preparation:** In each round, Alice randomly chooses a preparation basis $x \in \{0, 1\}$. Next, Alice chooses a uniformly random bit value $a \in \{0, 1\}$ as her raw data. Fred knows (x, a) and also uniformly at random chooses a state $|g_0\rangle$ or $|g_1\rangle$.
 - **Distribution:** In each round, if $|g_0\rangle$ chosen, Fred manipulates the source device to send $\tau_{x,a}$ to Bob through the insecure channel \mathcal{E} , if $|g_1\rangle$ chosen, Fred manipulates the source device to send $\bar{\tau}_{x,a}$ to Bob through the insecure channel $\bar{\mathcal{E}}$.
 - **Measurement:** In each round, Bob randomly chooses a measurement basis $y \in \{0, 1\}$, measurement device performs the projective measurements B_y , and then outputs a bit value $b \in \{0, 1\}$ as Bob's raw data.
 - **Collaboration:** In each round, Fred sends the ancillary system E to Eve as well as the state $|g_0\rangle$ or $|g_1\rangle$.
 - **Parameter estimation:** Same as the mirrored protocol.
 - **Key generation:** Same as the mirrored protocol.
 - **Post-processing:** Same as the mirrored protocol.
-

Corollary 1. *In the symmetrized protocol, Alice and Bob will obtain the same Q and W as that of the actual protocol, Eve will obtain the same information knowledge as that of the actual protocol.*

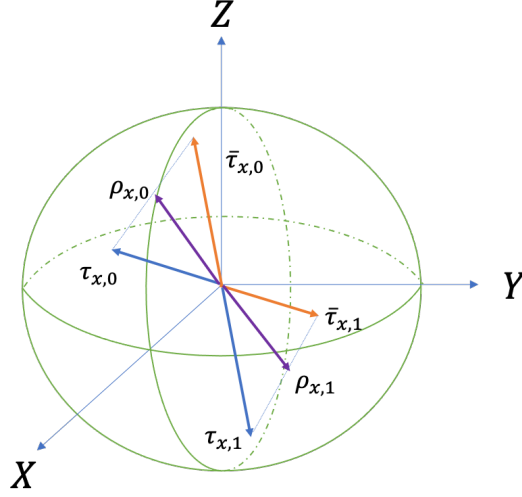


FIG. 10. The geometric relations between $\tau_{x,a}$, $\bar{\tau}_{x,a}$ and $\rho_{x,a}$ for each combination (x, a) .

Proof. Based on Lemma 3, the bit error of the actual protocol and mirrored protocol are same, by convex-linearity, the bit error of symmetrized protocol is same as that of the actual protocol, so that the W wouldn't change either. Based on the Eq. (42) and Eq. (44) in Lemma 4, the state after implementing B_0 is given by

$$\rho_{ABEG} = \frac{1}{2}(\rho_{ABE} \otimes |g_0\rangle\langle g_0| + \bar{\rho}_{ABE} \otimes |g_1\rangle\langle g_1|), \quad (48)$$

where the ancillary systems E and G are hold by Eve, so that Eve's information gain wouldn't change, which completes the proof. \square

In order to construct the reduced EB protocol, we need to renormalize the symmetrized protocol, which means reducing the two channels \mathcal{E} and $\bar{\mathcal{E}}$ to one channel, like the case of the actual protocol. Therefore, we introduce a renormalized protocol, the brief picture is showed in Fig. 11. In the renormalized protocol, Fred also knows (x, a) and manipulates the source device to send pure states $\{|\psi_{x,a}\rangle\}$ out, where $\{|\psi_{x,a}\rangle\}$ being basis-independent that of $|\psi_{0,0}\rangle\langle\psi_{0,0}| + |\psi_{0,1}\rangle\langle\psi_{0,1}| = |\psi_{1,0}\rangle\langle\psi_{1,0}| + |\psi_{1,1}\rangle\langle\psi_{1,1}| = I$, $|\psi_{x,a}\rangle$ go through a lossless channel \mathcal{F} and become $\{\rho_{x,a}\}$, then Fred applies a mixed channel of \mathcal{E} and $\bar{\mathcal{E}}$ denoted as \mathcal{E}_{mix} , so that $\{\rho_{x,a}\}$ become

$$\rho_{x,a}^e := \frac{Y_{x,a}\tau_{x,a}^e + \bar{Y}_{x,a}\bar{\tau}_{x,a}^e}{Y_{x,a} + \bar{Y}_{x,a}}, \quad (49)$$

after that, Fred respectively sends $\{\rho_{x,a}^e\}$ to Bob and all ancillary systems to Eve, and Bob performs projective measurements $\{B_y\}$. The details of the renormalized protocol are as showed in Tab. IV.

TABLE IV. The renormalized protocol

-
- **State preparation:** In each round, Alice randomly chooses a preparation basis $x \in \{0, 1\}$. Next, Alice chooses a uniformly random bit value $a \in \{0, 1\}$ as her raw data. Freds knows (x, a) and prepares *basis-independent* pure states $|\psi_{x,a}\rangle$.
 - **Distribution:** In each round, Fred manipulates the source device to send $|\psi_{x,a}\rangle$ to Bob through a *specific* and insecure channel controlled by Fred, which is described as $\mathcal{E}_{\text{mix}} \circ \mathcal{F}$.
 - **Measurement:** In each round, Bob randomly chooses a measurement basis $y \in \{0, 1\}$. Measurement device performs projective measurements B_y , and then, outputs a bit value $b \in \{0, 1\}$ as Bob's raw data.
 - **Collaboration:** In each round, Fred sends all ancillary systems to Eve.
 - **Parameter estimation:** Same as the mirrored protocol.
 - **Key generation:** Same as the mirrored protocol.
 - **Post-processing:** Same as the mirrored protocol.
-

Following the same argument, we shall prove that the renormalized protocol provides Alice and Bob the same statistics, and Eve at least the same information gain as or maybe more. To do this, we still refer to Choi–Jamiołkowski

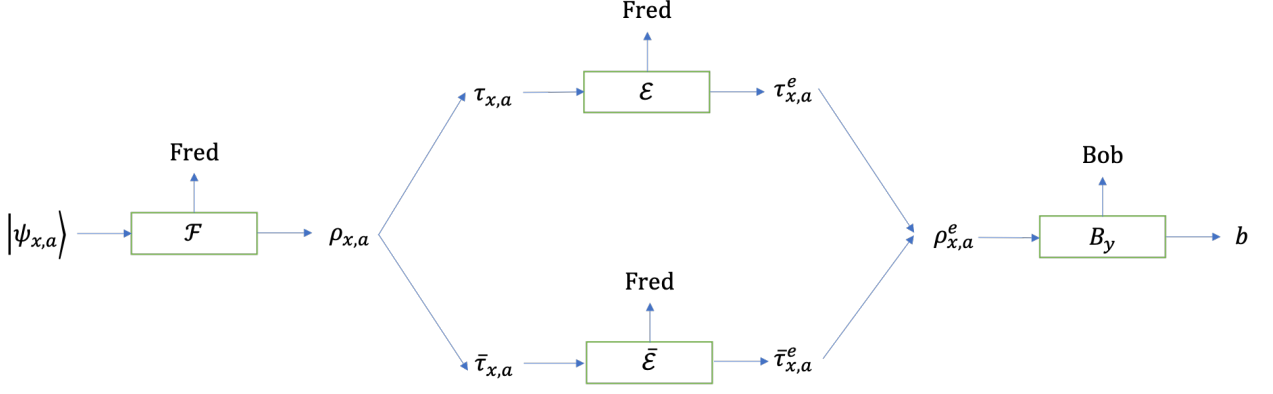


FIG. 11. The brief picture of the renormalized protocol.

isomorphism and Stinespring dilation picture. Let $U_{\mathcal{F}}$ on the system B , two-dimensional ancillary system F and G be the corresponding unitary transformation of \mathcal{F} , then $U_{\mathcal{F}}$ can be specified by the non-normalized state

$$|\Phi\rangle_{ABFG} := U_{\mathcal{F}}(|00\rangle_{AB} + |11\rangle_{AB})|f\rangle_F|g\rangle_G, \quad (50)$$

where $|f\rangle_F$ and $|g\rangle_G$ are the initial states of system F and G , respectively. Recalling Eq. (28), for each (x, a) , we denote

$$\begin{aligned} |\phi_{x,a}\rangle_{BF} &:= \sqrt{\mu_{x,a}}|\mu_{x,a}\rangle|f_0\rangle + \sqrt{\nu_{x,a}}|\nu_{x,a}\rangle|f_1\rangle \\ |\bar{\phi}_{x,a}\rangle_{BF} &:= \sqrt{\mu_{x,a}}|\nu_{x,a}\rangle|f_0\rangle + \sqrt{\nu_{x,a}}|\mu_{x,a}\rangle|f_1\rangle, \end{aligned} \quad (51)$$

as the Schmidt purifications of $\tau_{x,a}$ and $\bar{\tau}_{x,a}$, respectively, where $|f_0\rangle$ and $|f_1\rangle$ are the mutually orthogonal states of system F . Then we are ready to prove the existence of $|\psi_{x,a}\rangle$ and \mathcal{F} that $\mathcal{F}(|\psi_{x,a}\rangle\langle\psi_{x,a}|) = \rho_{x,a}$ for each (x, a) .

Lemma 5. *In the renormalized protocol, there exists pure qubit states $\{|\psi_{x,a}\rangle\}$ that $|\psi_{0,0}\rangle\langle\psi_{0,0}| + |\psi_{0,1}\rangle\langle\psi_{0,1}| = |\psi_{1,0}\rangle\langle\psi_{1,0}| + |\psi_{1,1}\rangle\langle\psi_{1,1}| = I$ and $|\Phi\rangle_{ABFG}$ that*

$$\mathcal{F}(|\psi_{x,a}\rangle\langle\psi_{x,a}|) = \text{Tr}_{AFG}[|\psi_{x,a}^*\rangle_A\langle\psi_{x,a}^*|\Phi\rangle_{ABFG}\langle\Phi|] = \rho_{x,a} \quad (52)$$

for each (x, a) . Moreover,

$$\begin{aligned} \text{Tr}\left[|\psi_{x,a}^*\rangle_A\langle\psi_{x,a}^*|\otimes|g_0\rangle\langle g_0|\Phi\rangle_{ABFG}\langle\Phi|\right] &= |\phi_{x,a}\rangle_{BF}\langle\phi_{x,a}| \\ \text{Tr}\left[|\psi_{x,a}^*\rangle_A\langle\psi_{x,a}^*|\otimes|g_1\rangle\langle g_1|\Phi\rangle_{ABFG}\langle\Phi|\right] &= |\bar{\phi}_{x,a}\rangle_{BF}\langle\bar{\phi}_{x,a}|, \end{aligned} \quad (53)$$

which means that the states $|g_0\rangle$ and $|g_1\rangle$ respectively encode channels \mathcal{E} and $\bar{\mathcal{E}}$, and is useful for the construction of the channel \mathcal{E}_{mix} .

Proof. Let the mutually orthogonal states $|\psi_{x,a}\rangle$ be the emitted states for each basis x in the renormalized protocol, and a corresponding channel \mathcal{F}_x specified by the non-normalized state

$$|\Phi_x\rangle_{ABFG} := \frac{1}{\sqrt{2}}\sum_{a=0}^1|\psi_{x,a}^*\rangle_A(|\phi_{x,a}\rangle_{BF}|g_0\rangle + |\bar{\phi}_{x,a}\rangle_{BF}|g_1\rangle) \quad (54)$$

where $|\psi_{x,a}^*\rangle_A$ are the complex conjugate of $|\psi_{x,a}\rangle$, then inserting Eq. (51), it is easy to verify that

$$\begin{aligned} \mathcal{F}_x(|\psi_{x,a}\rangle\langle\psi_{x,a}|) &= \text{Tr}_{AFG}[|\psi_{x,a}^*\rangle_A\langle\psi_{x,a}^*|\Phi_x\rangle_{ABFG}\langle\Phi_x|] \\ &= \frac{1}{2}(\text{Tr}_F[|\phi_{x,a}\rangle_{BF}\langle\phi_{x,a}| + \text{Tr}_F[|\bar{\phi}_{x,a}\rangle_{BF}\langle\bar{\phi}_{x,a}|]) \\ &= \frac{1}{2}(\tau_{x,a} + \bar{\tau}_{x,a}) \\ &= \rho_{x,a}, \end{aligned} \quad (55)$$

where we make use of fact that $|g_0\rangle$ and $|g_1\rangle$ are mutually orthogonal. Now, we already find such channels \mathcal{F}_x that $\mathcal{F}_x(|\psi_{x,a}\rangle\langle\psi_{x,a}|) = \rho_{x,a}$, then need to find such $\{|\psi_{x,a}\rangle\}$ that $|\Phi_0\rangle_{ABFG} = |\Phi_1\rangle_{ABFG}$. To accomplish this, we define that

$$|\xi_{x,a}\rangle := \frac{1}{\sqrt{2}}(|\phi_{x,a}\rangle_{BF}|g_0\rangle + |\bar{\phi}_{x,a}\rangle_{BF}|g_1\rangle), \quad (56)$$

of composite system BFG , and show that the two states $|\xi_{x,0}\rangle$ and $|\xi_{x,1}\rangle$ are mutually orthogonal for each x . We can make use of the freedom of the global phase of $|\mu_{x,1}\rangle$ and $|\nu_{x,1}\rangle$, and without loss of generality set $|\mu_{x,1}\rangle = \cos\theta_x|\mu_{x,0}\rangle + \sin\theta_x|\nu_{x,0}\rangle$ and $|\nu_{x,1}\rangle = \sin\theta_x|\mu_{x,0}\rangle - \cos\theta_x|\nu_{x,0}\rangle$ for some real number θ_x , so that $\langle\mu_{x,0}|\mu_{x,1}\rangle + \langle\nu_{x,0}|\nu_{x,1}\rangle = 0$. Inserting Eq. (51), for each x , we have the inner product that

$$\langle\xi_{x,0}|\xi_{x,1}\rangle = \frac{1}{2}\langle\phi_{x,0}|\phi_{x,1}\rangle_{BF} + \langle\phi_{x,0}|\bar{\phi}_{x,1}\rangle_{BF} = \frac{1}{2}(\sqrt{\mu_{x,0}\mu_{x,1}} + \sqrt{\nu_{x,0}\nu_{x,1}})(\langle\mu_{x,0}|\mu_{x,1}\rangle + \langle\nu_{x,0}|\nu_{x,1}\rangle) = 0, \quad (57)$$

so that

$$|\Phi_x\rangle_{ABFG} = \sum_{a=0}^1 |\psi_{x,a}^*\rangle_A |\xi_{x,a}\rangle, \quad (58)$$

is written in the form of maximally entangled state regarding to system A and composite system BFG . Thus, it is easy to verify that, if setting

$$|\psi_{1,a}^*\rangle = \sum_{a'=0}^1 |\psi_{0,a'}^*\rangle \langle\xi_{1,a}|\xi_{0,a'}\rangle, \quad (59)$$

for each a ,

$$\begin{aligned} |\Phi_1\rangle_{ABFG} &= \sum_{a=0}^1 \sum_{a'=0}^1 |\psi_{0,a'}^*\rangle \langle\xi_{1,a}|\xi_{0,a'}\rangle |\xi_{1,a}\rangle \\ &= \sum_{a'=0}^1 |\psi_{0,a'}^*\rangle \left(\sum_{a=0}^1 |\xi_{1,a}\rangle \langle\xi_{1,a}| \right) |\xi_{0,a'}\rangle \\ &= \sum_{a'=0}^1 |\psi_{0,a'}^*\rangle |\xi_{0,a'}\rangle \\ &= |\Phi_0\rangle_{ABFG}. \end{aligned} \quad (60)$$

By setting

$$|\Phi\rangle_{ABFG} = |\Phi_0\rangle_{ABFG} = |\Phi_1\rangle_{ABFG}, \quad (61)$$

that is, $\mathcal{F} = \mathcal{F}_0 = \mathcal{F}_1$, we prove that $\mathcal{F}(|\psi_{x,a}\rangle\langle\psi_{x,a}|) = \rho_{x,a}$ holds for each (x, a) . By Eq. (54) and Eq. (61), we immediately see that

$$\begin{aligned} \langle\psi_{x,a}^*|_A \langle g_0|\Phi\rangle_{ABFG} &= |\phi_{x,a}\rangle_{BF} \\ \langle\psi_{x,a}^*|_A \langle g_1|\Phi\rangle_{ABFG} &= |\bar{\phi}_{x,a}\rangle_{BF}, \end{aligned} \quad (62)$$

which completes the proof. \square

Next, we come to the proof of the existence of such mixed channel \mathcal{E}_{mix} that $\mathcal{E}_{\text{mix}}(\rho_{x,a})/\text{Tr}[\mathcal{E}_{\text{mix}}(\rho_{x,a})] = \rho_{x,a}^e$, for each (x, a) . Let $U_{\mathcal{E}_{\text{mix}}}$ on the system B , system F and E be the corresponding unitary transformation of \mathcal{E}_{mix} , then $U_{\mathcal{E}_{\text{mix}}}U_{\mathcal{F}}$ can be specified by the non-normalized state

$$|\Phi\rangle_{ABEFG} := |\text{filter}\rangle \langle\text{filter}| U_{\mathcal{E}_{\text{mix}}}U_{\mathcal{F}}(|00\rangle_{AB} + |11\rangle_{AB}) |e\rangle_E |f\rangle_F |g\rangle_G. \quad (63)$$

where the meaning of operator $|\text{filter}\rangle \langle\text{filter}|$ is same as that of Eq. (40) and Eq. (41). Now, we are ready to prove.

Lemma 6. *Let*

$$U_{\mathcal{E}_{\text{mix}}} = U_{\mathcal{E}} \otimes |g_0\rangle\langle g_0| + U_{\bar{\mathcal{E}}} \otimes |g_1\rangle\langle g_1|, \quad (64)$$

then

$$\frac{\mathcal{E}_{\text{mix}}(\rho_{x,a})}{\text{Tr}[\mathcal{E}_{\text{mix}}(\rho_{x,a})]} = \rho_{x,a}^e. \quad (65)$$

Proof. Inserting Eq. (54), Eq. (61) and Eq. (64) into Eq. (63), we obtain

$$|\Phi\rangle_{ABEFG} = |\text{filter}\rangle\langle\text{filter}| \frac{1}{\sqrt{2}} \sum_{a=0}^1 |\psi_{x,a}^*\rangle_A (U_{\mathcal{E}} |\phi_{x,a}\rangle_{BF} |g_0\rangle + U_{\bar{\mathcal{E}}} |\bar{\phi}_{x,a}\rangle_{BF} |g_1\rangle) |e\rangle_E, \quad (66)$$

so that

$$\begin{aligned} \mathcal{E}_{\text{mix}}(\rho_{x,a}) &= \mathcal{E}_{\text{mix}} \circ \mathcal{F}(|\psi_{x,a}\rangle\langle\psi_{x,a}|) \\ &= \text{Tr}_{AEFG}[|\Phi\rangle_{ABEFG} \langle\Phi| \psi_{x,a}^*\rangle_A \langle\psi_{x,a}^*|] \\ &= \frac{1}{2} |\text{filter}\rangle\langle\text{filter}| \text{Tr}_{EFG}[P\{(U_{\mathcal{E}} |\phi_{x,a}\rangle_{BF} |g_0\rangle + U_{\bar{\mathcal{E}}} |\bar{\phi}_{x,a}\rangle_{BF} |g_1\rangle) |e\rangle_E\}] |\text{filter}\rangle\langle\text{filter}| \\ &= \frac{1}{2} |\text{filter}\rangle\langle\text{filter}| (\text{Tr}_E[U_{\mathcal{E}}(\tau_{x,a} \otimes |e\rangle_E \langle e|) U_{\mathcal{E}}^\dagger] + U_{\bar{\mathcal{E}}}(\bar{\tau}_{x,a} \otimes |e\rangle_E \langle e|) U_{\bar{\mathcal{E}}}^\dagger) |\text{filter}\rangle\langle\text{filter}| \\ &= \frac{1}{2} (\text{Tr}_{AE}[\tau_{x,a}^* |\Phi\rangle_{ABE} \langle\Phi|] + \text{Tr}_{AE}[\bar{\tau}_{x,a}^* |\bar{\Phi}\rangle_{ABE} \langle\bar{\Phi}|]) \\ &= \frac{1}{2} [\mathcal{E}(\tau_{x,a}) + \bar{\mathcal{E}}(\bar{\tau}_{x,a})] \\ &= \frac{1}{2} (Y_{x,a} \tau_{x,a}^e + \bar{Y}_{x,a} \bar{\tau}_{x,a}^e) \end{aligned} \quad (67)$$

for each (x, a) , where we make use of Eq. (51) in the fourth equation, Eq. (40) and Eq. (41) in the fifth equation. According to the definition of $\rho_{x,a}^e$ in Eq. (49), we immediately complete the proof. \square

Corollary 2. *In the renormalized protocol, Fred will provide Alice and Bob the same Q and W as that of the actual protocol.*

Proof. In the renormalized protocol, the statistics are totally same as that of the symmetrized protocol, by Corollary 1, we complete the proof. \square

Next, we come to the evaluation of Eve's information gain in the renormalized protocol, as the following lemma shows.

Lemma 7. *In the renormalized protocol, Fred will provide Eve more information knowledge than or at least the same as that of the actual protocol.*

Proof. Following the same argument in the Lemma 2, if considering the key generation basis $x = y = 0$ only, the state after implementing B_0 is given by

$$\rho_{ABEFG} = \sum_{a,b=0}^1 |ab\rangle_{AB} \langle ab| \otimes \rho_{EFG|a,b}, \quad (68)$$

where

$$\rho_{EFG|a,b} = \text{Tr}_{AB}[(|\psi_{0,a}^*\rangle_A \langle\psi_{0,a}^*| \otimes B_{b|0}) |\Phi\rangle_{ABEFG} \langle\Phi|], \quad (69)$$

for each (a, b) , and Eve holds the ancillary systems E , F and G . Then, inserting Eq. (66) and following the same evolution of Eq. (67), we have

$$\begin{aligned} |g_0\rangle\langle g_0| \text{Tr}_F[\rho_{EFG|a,b} |g_0\rangle\langle g_0|] &= \frac{1}{2} |\text{filter}\rangle\langle\text{filter}| \text{Tr}_F[P\{B_{b|0} U_{\mathcal{E}} |\phi_{0,a}\rangle_{BF}\}] |\text{filter}\rangle\langle\text{filter}| \otimes |g_0\rangle\langle g_0| \\ &= \frac{1}{2} |\text{filter}\rangle\langle\text{filter}| B_{b|0} U_{\mathcal{E}}(\tau_{0,a} \otimes |e\rangle_E \langle e|) U_{\mathcal{E}}^\dagger |\text{filter}\rangle\langle\text{filter}| \otimes |g_0\rangle\langle g_0| \\ &= \frac{1}{2} \text{Tr}_{AB}[(\tau_{0,a}^* \otimes B_{b|0}) |\Phi\rangle_{ABE} \langle\Phi|] \otimes |g_0\rangle\langle g_0| \\ &= \frac{1}{2} \rho_{E|a,b} \otimes |g_0\rangle\langle g_0|, \end{aligned} \quad (70)$$

where we make use of Eq. (43), and similarly,

$$\begin{aligned} |g_1\rangle\langle g_1| \text{Tr}_F[\rho_{EFG|a,b}] |g_1\rangle\langle g_1| &= \frac{1}{2} \text{Tr}_{AB}[(\bar{\tau}_{0,a}^* \otimes M_0) |\bar{\Phi}\rangle_{ABE} \langle\bar{\Phi}|] \otimes |g_1\rangle\langle g_1| \\ &= \frac{1}{2} \bar{\rho}_{E|a,b} \otimes |g_1\rangle\langle g_1|, \end{aligned} \quad (71)$$

where we make use of Eq. (45). Considering ρ_{ABE} in Eq. (42), $\bar{\rho}_{ABE}$ in Eq. (44) and ρ_{ABEG} in Eq. (48), we find that

$$(|g_0\rangle\langle g_0| + |g_1\rangle\langle g_1|) \text{Tr}_{FH}[\rho_{ABEFG}] (|g_0\rangle\langle g_0| + |g_1\rangle\langle g_1|) = \rho_{ABEG}, \quad (72)$$

that is, ρ_{ABEG} is attainable by discarding system F followed by a projective measurement on system G with basis $\{|g_0\rangle, |g_1\rangle\}$. Due to *data processing inequality*, such operation wouldn't increase Eve's information gain. As a result, Eve's information gain in the renormalized protocol is more than or at least the same as that of the symmetrized protocol, by Corollary 1, we complete the proof. \square

Now, we are ready to introduce the reduced EB protocol, as showed in Tab. V. Here, we emphasize that the reduced EB protocol provides Alice and Bob the same observable statistics, and Eve more information knowledge than or at least the same as that of the actual protocol. In other words, the reduced EB protocol may pessimistically result in lower key rate than that of actual protocol. Since the emitted states are *basis-independent* that of $|\psi_{0,0}\rangle\langle\psi_{0,0}| + |\psi_{0,1}\rangle\langle\psi_{0,1}| = |\psi_{1,0}\rangle\langle\psi_{1,0}| + |\psi_{1,1}\rangle\langle\psi_{1,1}| = I$ in the renormalized protocol, thus, in the reduced EB protocol, we can remove Eve's collaborator, Fred, and equivalently view that the specific and insecure channel $\mathcal{E}_{\text{mix}} \circ \mathcal{F}$ is controlled by Eve. Moreover, we equivalently view that Alice prepares the Bell state $(|00\rangle + |11\rangle)/\sqrt{2}$, and send the second qubit to Bob through the channel, after Bob receives it, Alice performs the projective measurement $A_x = |\psi_{x,0}^*\rangle\langle\psi_{x,0}^*| - |\psi_{x,1}^*\rangle\langle\psi_{x,1}^*|$ on the first qubit and Bob performs B_y on the second qubit to collect data. For simplicity, in the following discussion, we rephrase the composite ancillary system EFG as E in the reduced EB protocol.

TABLE V. **The reduced entanglement-based protocol**

-
- **State preparation:** In each round, Alice prepares the Bell state $(|00\rangle + |11\rangle)/\sqrt{2}$.
 - **Distribution:** In each round, Alice sends the second qubit to Bob through a specific and insecure channel controlled by Eve, which is described as $\mathcal{E}_{\text{mix}} \circ \mathcal{F}$.
 - **Measurement:** In each round, Alice (Bob) randomly chooses a measurement basis $x(y) \in \{0, 1\}$. Measurement device performs an uncharacterized measurements $A_x(B_y)$, and then, outputs a bit value $a(b) \in \{0, 1\}$ as Alice's (Bob's) raw data.
 - **Parameter estimation:** Same as the mirrored protocol.
 - **Key generation:** Same as the mirrored protocol.
 - **Post-processing:** Same as the mirrored protocol.
-

Step 2: Connecting Quantum Discord to Information Leakage.

For the security analysis against collective attack in EB version, we make use of Devetak-Winter bound [43] to calculate the key rate, which is given by

$$R \geq H(A_0|E) - h(Q), \quad (73)$$

where $H(A_0|E)$ is variable a 's entropy conditional on Eve's system if performing A_0 . The information leakage captured by the mutual information is then given by $I(A_0 : E) := H(A_0) - H(A_0|E) = 1 - H(A_0|E)$ where we use the fact that the variable a 's entropy $H(A_0) = 1$. Clearly, the term of $H(A_0|E)$ is directly related to the information leakage. To estimate the lower bound of $H(A_0|E)$, we shall consider the form of two qubit state ρ_{AB} before measurements.

Lemma 8. *In the reduced EB protocol, we can reduce ρ_{AB} to a Bell-diagonal state given by*

$$\rho_{AB} = \lambda_1 |\Phi^+\rangle\langle\Phi^+| + \lambda_2 |\Phi^-\rangle\langle\Phi^-| + \lambda_3 |\Psi^+\rangle\langle\Psi^+| + \lambda_4 |\Psi^-\rangle\langle\Psi^-|, \quad (74)$$

where $\lambda_1 \geq \lambda_2 \geq \lambda_3 \geq \lambda_4 \geq 0$ are some coefficients satisfying $\lambda_1 + \lambda_2 + \lambda_3 + \lambda_4 = 1$, $|\Phi^\pm\rangle := (|00\rangle \pm |11\rangle)/\sqrt{2}$ and $|\Psi^\pm\rangle := (|01\rangle \pm |10\rangle)/\sqrt{2}$ are four Bell states.

Proof. Following the argument in the main text, in order to prove that ρ_{AB} is Bell-diagonal, it is sufficient to prove that ρ_{AB} has maximally mixed marginals [40, 41]. In the reduced EB protocol, Alice's local qubit is always maximally mixed, that is, the reduced state $\rho_A = \text{Tr}_B[\rho_{AB}] = I/2$, since Eve never interferes her qubit. And it is straightforward to see that $\rho_B = \text{Tr}_A[\rho_{AB}] = I/2$ because

$$\rho_B = \frac{1}{2} \sum_{a=0}^1 \rho_{x,a}^e = \frac{1}{2} \sum_{a=0}^1 \frac{Y_{x,a} \tau_{x,a}^e + \bar{Y}_{x,a} \bar{\tau}_{x,a}^e}{Y_{x,a} + \bar{Y}_{x,a}} = \frac{I}{2}. \quad (75)$$

holds for each x . Finally, we shall prove that ρ_{AB} is a Bell-diagonal state with eigenvalues ordered as $\lambda_1 \geq \lambda_2 \geq \lambda_3 \geq \lambda_4$, if choosing proper local reference frame on both Alice's and Bob's sides [40, 41]. We recall the Bloch representation of ρ_{AB} , that is,

$$\rho_{AB} = \frac{1}{4} (I \otimes I + T_x \sigma_x \otimes \sigma_x + T_y \sigma_y \otimes \sigma_y + T_z \sigma_z \otimes \sigma_z), \quad (76)$$

where $T_z = \lambda_1 + \lambda_2 - \lambda_3 - \lambda_4$, $T_x = \lambda_1 - \lambda_2 + \lambda_3 - \lambda_4$ and $-T_y = \lambda_1 - \lambda_2 - \lambda_3 + \lambda_4$. To obtain the order $\lambda_1 \geq \lambda_2 \geq \lambda_3 \geq \lambda_4$, it is equivalent to have $|T_z| \geq |T_x| \geq |T_y|$. For the purpose of arranging these elements, we can perform the following unitary operation: 1) applying $H_{zx} := (\sigma_z + \sigma_x)/\sqrt{2}$ on both qubits if $|T_z| \leq |T_x|$, then we have $|T_z| \geq |T_x|$, 2) applying $H_{yz} := (\sigma_y + \sigma_z)/\sqrt{2}$ on both qubits if $|T_z| \leq |T_y|$, then we have $|T_z| \geq |T_y|$, 3) applying $H_{xy} := (\sigma_x + \sigma_y)/\sqrt{2}$ on both qubits if $|T_x| \leq |T_y|$, then we have $|T_x| \geq |T_y|$, till now, we have $|T_z| \geq |T_x| \geq |T_y|$, next, 4) doing nothing if $T_z \geq 0$ and $T_x \geq 0$, 5) applying σ_z on Bob's qubit if $T_z \geq 0$ and $T_x \leq 0$, 6) applying σ_x on Bob's qubit if $T_z \leq 0$ and $T_x \geq 0$, 7) applying σ_y on Bob's qubit if $T_z \leq 0$ and $T_x \leq 0$. Finally, by choosing a proper local reference on each side, we have $T_z \geq T_x \geq |T_y|$, or equivalently $\lambda_1 \geq \lambda_2 \geq \lambda_3 \geq \lambda_4$, which completes the proof. \square

In Ref. [18], the author has proved that the upper bound of information leakage i.e., the lower bound of $H(A_0|E)$ is directly related to QD by using Koashi-Winter relation [42]. Here, we provide an alternative and easier proof for the described Bell-diagonal state.

Lemma 9. *Let ρ_{AB} be captured by Eq. (74), then*

$$\min_{A_0} H(A_0|E) = D(B|A), \quad (77)$$

where the quantity of QD is defined in the main text.

Proof. As said in the main text, $D(B|A) = \min_{\{E_a\}} H(B|E_a) + H(A) - H(AB)$, where the minimization is over all POVMs $\{E_a\}$. Fortunately, for two-qubit Bell-diagonal state, it has been proved that it is sufficient to consider the minimization over all projective measurements [57–59]. Let $E_a = |\phi_a\rangle\langle\phi_a|$ be the orthogonal projectors where $a \in \{0, 1\}$, then the post-measurement state ρ'_{AB} is given by

$$\rho_{AB} \xrightarrow{E_a} \rho'_{AB} = \frac{1}{2} \sum_{a=0}^1 |\phi_a\rangle\langle\phi_a| \otimes \langle\phi_a| \rho_{AB} |\phi_a\rangle, \quad (78)$$

then we immediately have $H(E_a) = H(A) = 1$, where $H(E_b)$ and $H(B)$ are the von Neumann entropies for subsystems $\rho'_B = \text{Tr}_A[\rho'_{AB}]$ and $\rho_B = \text{Tr}_A[\rho_{AB}]$ respectively. Therefore the right hand side (r.h.s) of (77) becomes

$$\min_{\{E_a\}} H(E_a B) - H(AB), \quad (79)$$

where $H(E_a B) = H(B|E_a) + H(E_a)$ is the entropy for ρ'_{AB} . Then we consider the left hand side (l.h.s) of (77), let Eve hold the purification of ρ_{AB} , that is, the tripartite system hold by Alice, Bob and Eve is given by

$$|\Psi\rangle_{ABE} = \sqrt{\lambda_1} |\Phi^+\rangle |e_1\rangle + \sqrt{\lambda_2} |\Phi^-\rangle |e_2\rangle + \sqrt{\lambda_3} |\Psi^+\rangle |e_3\rangle + \sqrt{\lambda_4} |\Psi^-\rangle |e_4\rangle, \quad (80)$$

where $|e_1\rangle, |e_2\rangle, |e_3\rangle$ and $|e_4\rangle$ are mutually orthogonal with each other. Similarly, let $|\psi_a\rangle\langle\psi_a|$ be the orthogonal projectors corresponding to the measurement operator A_0 , then the post-measurement state $\rho_{A_0 E}$ is given by

$$|\Psi\rangle_{ABE} \langle\Psi| \rightarrow \rho_{A_0 E} = \frac{1}{2} \sum_{a=0}^1 |\psi_a\rangle\langle\psi_a| \otimes \text{Tr}_B[\langle\psi_a|\Psi\rangle_{ABE} \langle\Psi|\psi_a\rangle]. \quad (81)$$

Simultaneously, if tracing Eve's system out, we have the post-measurement state ρ_{A_0B} given by

$$|\Psi\rangle_{ABE} \langle\Psi| \rightarrow \rho_{A_0B} = \frac{1}{2} \sum_{a=0}^1 |\psi_a\rangle \langle\psi_a| \otimes \text{Tr}_E[\langle\psi_a|\Psi\rangle_{ABE} \langle\Psi|\psi_a\rangle]. \quad (82)$$

Since $|\Psi\rangle_{ABE}$ is pure, we have $H(A_0B) = H(A_0E)$ where $H(A_0B)$ and $H(A_0E)$ are the entropies of ρ_{A_0B} and ρ_{A_0E} respectively, then the l.h.s becomes

$$\min_{A_0} H(A_0B) - H(E), \quad (83)$$

where $H(E)$ is the entropy of $\rho_E = \text{Tr}_{AB}[|\Psi\rangle_{ABE} \langle\Psi|]$. By making use of the fact that $H(AB) = H(E)$, we immediately obtain that the l.h.s equals to the r.h.s, which completes the proof. \square

Corollary 3. *Let ρ_{AB} be captured by Eq. (74), then*

$$D(B|A) = 1 - (\lambda_1 + \lambda_2)h\left(\frac{\lambda_2}{\lambda_1 + \lambda_2}\right) - (\lambda_3 + \lambda_4)h\left(\frac{\lambda_4}{\lambda_3 + \lambda_4}\right), \quad (84)$$

with equality for $A_0 = \sigma_z$.

Proof. In Ref. [58], it has been proved that: provided a two-qubit Bell-diagonal states with the order $T_z \geq T_x \geq |T_y|$, we have

$$J(B|A) = 1 - h\left(\frac{1 + T_z}{2}\right) = 1 - h(\lambda_1 + \lambda_2), \quad (85)$$

where the definition of $J(B|A)$ can be found in the main text, and the equality holds with $A_0 = \sigma_z$. Therefore, we say that the best case for Eve is Bob performing $A_0 = \sigma_z$ measurement for key generation rounds. After the standard calculation procedure, the mutual information of ρ_{AB} is given by

$$\begin{aligned} I(A : B) &= H(A) + H(B) - H(AB) \\ &= 2 - h(\lambda_1 + \lambda_2) - (\lambda_1 + \lambda_2)h\left(\frac{\lambda_2}{\lambda_1 + \lambda_2}\right) - (\lambda_3 + \lambda_4)h\left(\frac{\lambda_4}{\lambda_3 + \lambda_4}\right). \end{aligned} \quad (86)$$

Then, we have

$$\begin{aligned} D(B|A) &= I(A : B) - J(B|A) \\ &= 1 - (\lambda_1 + \lambda_2)h\left(\frac{\lambda_2}{\lambda_1 + \lambda_2}\right) - (\lambda_3 + \lambda_4)h\left(\frac{\lambda_4}{\lambda_3 + \lambda_4}\right), \end{aligned} \quad (87)$$

which completes the proof. \square

Step 3: Obtaining the Lower Bound of Secure Key Rate.

Lemma 10. *Let W_{\max} be the maximal achievable witness [21] of ρ_{AB} in Eq. (74), then*

$$D(B|A) \geq 1 - h\left(\frac{1 - W_{\max}}{2}\right), \quad (88)$$

with equality if and only if $\lambda_3 = \lambda_4 = 0$.

Proof. In the main text, we have reviewed the QD witness defined in [21], and we will further simplify its form in our case. Considering the Bell-diagonal state in Eq. (74) and some projective measurements A_x and B_y , we have $\langle A_x \rangle = \langle B_y \rangle = 0$, and $Q_{xy} = \langle A_x \otimes B_y \rangle$, where

$$\begin{aligned} \langle A_x \rangle &= \text{Tr}[\rho_A A_x] = \text{Pr}[a = 0|x] - \text{Pr}[a = 1|x], \\ \langle B_y \rangle &= \text{Tr}[\rho_B B_y] = \text{Pr}[b = 0|y] - \text{Pr}[b = 1|y], \\ \langle A_x \otimes B_y \rangle &= \text{Tr}[\rho_{AB} A_x \otimes B_y] = \text{Pr}[a = b|xy] - \text{Pr}[a \neq b|xy], \end{aligned} \quad (89)$$

according to the definitions in the main text, and then

$$W = \begin{vmatrix} Q_{00} & Q_{01} \\ Q_{10} & Q_{11} \end{vmatrix} = \begin{vmatrix} \langle A_0 \otimes B_0 \rangle & \langle A_0 \otimes B_1 \rangle \\ \langle A_1 \otimes B_0 \rangle & \langle A_1 \otimes B_1 \rangle \end{vmatrix}. \quad (90)$$

We recall that the maximum of QD witness happens when A_x ($x \in \{0, 1\}$) are mutually orthogonal basis (MUB) measurements as well as B_y ($y \in \{0, 1\}$) [21], and in our case, the corresponding Bloch vectors should lie in the X - Z plane of Bloch sphere. In other words, to achieve W_{\max} and $J(B|A)$ in Eq. (85), Bob should choose $A_0 = \sigma_z$ and $A_1 = \sigma_x$, and Alice should choose $B_0 = \cos \varphi \sigma_z - \sin \varphi \sigma_x$ and $B_1 = \sin \varphi \sigma_z + \cos \varphi \sigma_x$ with any angle φ . Here we can freely choose the angle φ since it wouldn't change the determinant [26]. Therefore, the EB version of standard BB84 protocol is captured by $\varphi = 0$, and is one of special case to achieve W_{\max} in our protocol. Since we have proved that the maximal achievable witness $W_{\max} = T_z T_x$ (see Eq. (10) in Ref. [21]), then

$$\begin{aligned} D(B|A) &= 1 - (\lambda_1 + \lambda_2)h\left(\frac{\lambda_2}{\lambda_1 + \lambda_2}\right) - (\lambda_3 + \lambda_4)h\left(\frac{\lambda_4}{\lambda_3 + \lambda_4}\right) \\ &\geq 1 - h(\lambda_2 + \lambda_4) \\ &= 1 - h\left(\frac{1 - T_x}{2}\right) \\ &\geq 1 - h\left(\frac{1 - W_{\max}}{2}\right), \end{aligned} \tag{91}$$

where the first inequality holds since the binary entropy function is strictly concave, and the second inequality holds since $T_x \geq W_{\max}$ and the binary entropy function is monotonically increasing in the interval $[0, 1/2]$, and it is straightforward to see that the condition of equality is $T_z = 1$, that is, $\lambda_3 = \lambda_4 = 0$, which completes the proof. \square

Theorem 1. *The secret key rate against collective attack of DB-QKD is given by*

$$R \geq 1 - h(Q) - h\left(\frac{1 - W}{2}\right), \tag{92}$$

where

$$W = \begin{vmatrix} 1 - 2e_{00} & 1 - 2e_{01} \\ 1 - 2e_{10} & 1 - 2e_{11} \end{vmatrix}, \tag{93}$$

is the observed QD witness based on PM version.

Proof. For each (x, y) , we have already proved that the renormalized protocol provides the same bit error as that of the actual protocol in Corollary 2, thus, the reduced EB protocol also provides the same bit error, specifically, $\langle A_x \otimes B_y \rangle = 1 - 2e_{xy}$. Therefore, in the reduced EB protocol, we have

$$W = \begin{vmatrix} 1 - 2e_{00} & 1 - 2e_{01} \\ 1 - 2e_{10} & 1 - 2e_{11} \end{vmatrix} = \begin{vmatrix} \langle A_0 \otimes B_0 \rangle & \langle A_0 \otimes B_1 \rangle \\ \langle A_1 \otimes B_0 \rangle & \langle A_1 \otimes B_1 \rangle \end{vmatrix} \leq W_{\max}. \tag{94}$$

Owing to Lemma 9, Corollary 3 and Lemma 10, we have

$$\min_{A_0} H(A_0|E) = D(B|A) \geq 1 - h\left(\frac{1 - W_{\max}}{2}\right) \geq 1 - h\left(\frac{1 - W}{2}\right), \tag{95}$$

where the last inequality holds since the binary entropy function is monotonically increasing in the interval $[0, 1/2]$. Finally, owing to the Devetak-Winter bound, the secret key rate is given by

$$R \geq H(A_0|E) - h(Q) \geq \min_{A_0} H(A_0|E) - h(Q) \geq 1 - h(Q) - h\left(\frac{1 - W}{2}\right), \tag{96}$$

which completes the proof. \square

C. Decoy-state DB-QKD with finite data effects

DB-QKD needs to calculate the QD witness according to the following equation,

$$W = \begin{vmatrix} 1 - 2e_{1|ZZ} & 1 - 2e_{1|ZX} \\ 1 - 2e_{1|XZ} & 1 - 2e_{1|XX} \end{vmatrix}, \tag{97}$$

where e_1 is the single-photon error rate, the superscript represents basis choice of Alice and Bob. Using weak coherent source, we cannot measure e_1 directly, they can only be estimated by the decoy-state method. So W should be minimized by

$$\begin{aligned} \min W &= \begin{vmatrix} 1 - 2e_{1|ZZ} & 1 - 2e_{1|ZX} \\ 1 - 2e_{1|XZ} & 1 - 2e_{1|XX} \end{vmatrix}, \\ \text{s.t.} & \begin{cases} e_{1|ZZ}^L \leq e_{1|ZZ} \leq e_{1|ZZ}^U \\ e_{1|ZX}^L \leq e_{1|ZX} \leq e_{1|ZX}^U \\ e_{1|XZ}^L \leq e_{1|XZ} \leq e_{1|XZ}^U \\ e_{1|XX}^L \leq e_{1|XX} \leq e_{1|XX}^U \end{cases}, \end{aligned} \quad (98)$$

where the superscripts ‘L’ and ‘U’ represent the lower bound and upper bound, respectively. The above equation shows that, to obtain W , all click events are preserved regardless of whether their bases are matched, then used to calculate the upper bound and lower bound of e_1 . According to the three-intensity decoy-state method, e_1^L and e_1^U can be obtained by [29–32]

$$\begin{aligned} e_1^L &= \frac{e^\nu EQ_\nu^L - e^\omega EQ_\omega^U - \frac{\nu^2 - \omega^2}{\mu^2} (EQ_\mu^U e^\mu - e_0 Y_0^L)}{(\nu - \omega - \frac{\nu^2 - \omega^2}{\mu}) Y_1^U}, \\ e_1^U &= \min \left\{ \frac{EQ_\nu^U e^\nu - EQ_\omega^L e^\omega}{(\nu - \omega) Y_1^L}, \frac{EQ_\mu^U e^\mu - EQ_\omega^L e^\omega}{(\mu - \omega) Y_1^L}, \frac{EQ_\mu^U e^\mu - EQ_\nu^L e^\nu}{(\mu - \nu) Y_1^L} \right\}, \end{aligned} \quad (99)$$

where μ, ν, ω are the intensity of phase-randomized weak coherent states, Q_μ, Q_ν, Q_ω are correspondingly the gain of different intensities, $EQ_\mu, EQ_\nu, EQ_\omega$ are correspondingly the error of different intensities, and Y_1^L and Y_1^U are respectively the lower bound and upper bound of the single-photon yield, and they can be derived from

$$\begin{aligned} Y_1^L &= \frac{\mu}{\mu\nu - \mu\omega - \nu^2 + \omega^2} \left(Q_\nu^L e^\nu - Q_\omega^U e^\omega - \frac{\nu^2 - \omega^2}{\mu^2} (Q_\mu^U e^\mu - Y_0^L) \right), \\ Y_1^U &= \min \left\{ \frac{Q_\mu^U e^\mu - Y_0^L}{\mu}, \frac{Q_\nu^U e^\nu - Y_0^L}{\nu}, \frac{Q_\omega^U e^\omega - Y_0^L}{\omega}, \frac{Q_\mu^U e^\mu - Q_\omega^L e^\omega}{\mu - \omega}, \frac{Q_\nu^U e^\nu - Q_\omega^L e^\omega}{\nu - \omega}, \frac{Q_\mu^U e^\mu - Q_\nu^L e^\nu}{\mu - \nu} \right\}, \end{aligned} \quad (100)$$

where Y_0^L is the lower bound of yield for vacuum state, which is given by

$$Y_0^L = \max \left\{ \frac{\nu Q_\omega^L e^\omega - \omega Q_\nu^U e^\nu}{\nu - \omega}, \frac{\mu Q_\omega^L e^\omega - \omega Q_\mu^U e^\mu}{\mu - \omega}, \frac{\nu Q_\omega^L e^\omega - \omega Q_\nu^U e^\nu}{\nu - \omega}, 0 \right\}. \quad (101)$$

The superscripts L and U represent the lower bound and upper bound, respectively, which can be obtained by the Chernoff bound as shown in Eq. (102). Based on the Q_μ, Q_ν, Q_ω and $EQ_\mu, EQ_\nu, EQ_\omega$ observed in every combination of basis, the corresponding e_1^L and e_1^U can be obtained, then W can be minimized based on Eq. (98).

Fig. 12 shows the comparisons of secure key rates in the three cases, all parameters are optimized for the sake of fairness. The total number, n_Z , is defined as the counts in Z basis and the failure probability is set to 10^{-9} . Compared with previous protocols based on the phase error, the difference of DB-QKD protocol in key generation is the QD witness. The QD witness is a minimized value of the witness determinant. To obtain the minimum value, eight bounds of the single-photon errors should be calculated, where each bound is obtained by the decoy-state method. More bounds enhance the finite-size effects, so a degradation of the witness is observed, which leads to a reduction of secure key rates.

D. Experimental data

In this section, the experimental data are listed as following tables. In all tables, n and m represent the number of successful events and the number of error events, where the superscripts ‘L’ and ‘U’ represent the lower bound and upper bound, respectively. The bounds are obtained by the multiplicative Chernoff bound,

$$\begin{aligned} \bar{X}^L &= \frac{X}{1 + \delta^L}, \\ \bar{X}^U &= \frac{X}{1 - \delta^U}, \end{aligned} \quad (102)$$

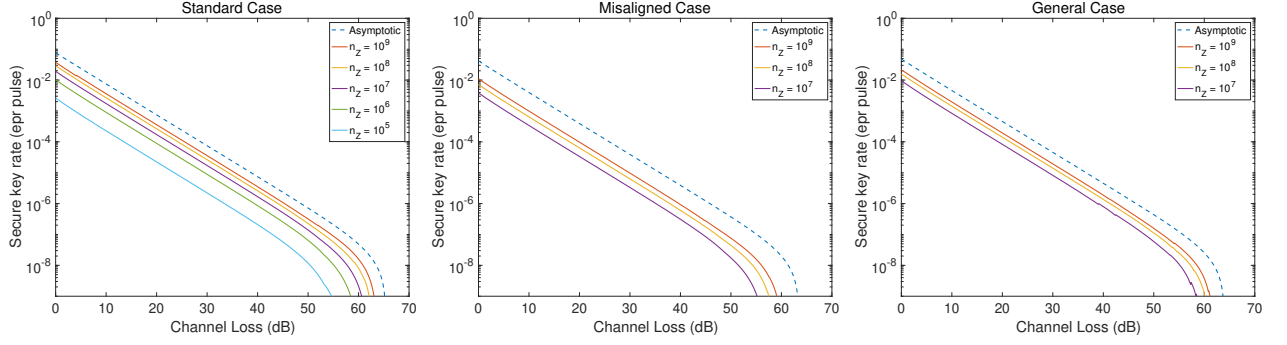


FIG. 12. The comparisons of secure key rates between the asymptotic and finite-size situations

where X is an observable, δ^L and δ^U can be obtained by the simplified forms [60]

$$\delta^L = \delta^U = \frac{3\beta + \sqrt{8\beta X + \beta^2}}{2(X - \beta)}, \quad (103)$$

which requires $X \geq 6\beta$. $\beta = -\ln(\epsilon/2)$ and $\epsilon = 10^{-9}$. For some observables that not meets the condition, we solve the δ^L and δ^U by

$$\begin{aligned} e^{-\frac{\delta^2 X}{2(1-\delta^U)}} &= \frac{\epsilon}{2}, \\ e^{-\frac{\delta^2 X}{4(1+\delta^L)}} &= \frac{\epsilon}{2}. \end{aligned} \quad (104)$$

Tabs. VI and VII shows the data obtained in the standard case. The upper bound of information leakage in DB-QKD is $h(\frac{1-W}{2})$, the upper bound of information leakage in BB84 is $h(e_1)$ [43]. Here, the terms of $(1-W)/2$ and e_1 are 1.69×10^{-2} and 5.05×10^{-3} , respectively, resulting secret key rates of 4.46×10^{-4} and 4.36×10^{-4} .

Tabs. VIII-IX and X list the data collected in the misaligned case where the phase reference frame of Alice and Bob is misaligned with $\pi/9$ and $2\pi/9$. The term of $(1-W)/2$ and secret key rate of DB-QKD are 2.21×10^{-2} and 2.43×10^{-4} for $\theta = \pi/9$, respectively, and are 2.79×10^{-2} and 3.36×10^{-5} for $\theta = 2\pi/9$. Because BB84 cannot generate key when rotating $2\pi/9$, Tab. X only shows the data of DB-QKD, the corresponding e_1 and secret key rate are 3.98×10^{-2} and 1.86×10^{-4} , respectively.

In the general case, following the representative example in the main text, the mixed qubit states prepared by Alice are given by

$$\tau_{x,a} = \frac{1}{4}P\{|s\rangle + (i)^x(-1)^a|l\rangle\} + \frac{1}{4}P\{|s\rangle + (i)^x(-1)^a e^{i\pi/9}|l\rangle\}, \quad (105)$$

where $P\{x\} := |x\rangle\langle x|$. The elements of POVMs conducted by Bob are given by

$$M_{b|y} = \frac{1}{4}P\{|s\rangle + (i)^y(-1)^b|l\rangle\} + \frac{1}{4}P\{|s\rangle + (i)^y(-1)^b e^{i\pi/9}|l\rangle\}. \quad (106)$$

The corresponding experimental data are shown in Tab. XI. The term of $(1-W)/2$ and secret key rate in this case are 5.27×10^{-2} and 2.07×10^{-4} , respectively.

In our experimental design, we choose three specific examples to respectively represent standard case, misaligned case and general case. To figuratively show the example of general case, in Fig. 13, we show the geometric relationship between the three specific examples.

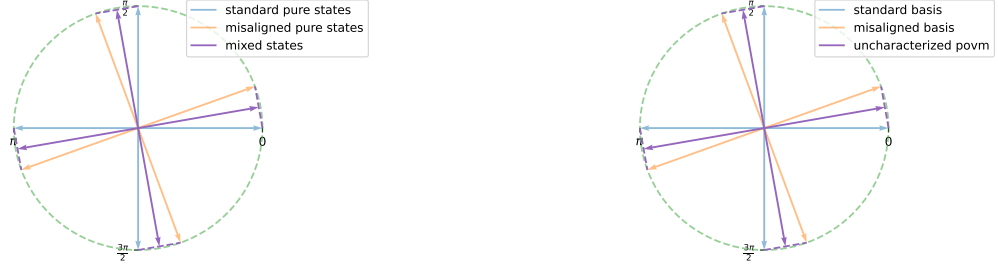


FIG. 13. The mixed states and the POVMs for general case

TABLE VI. Experimental data of DB-QKD in the standard case ($\theta = 0$).

$\mu = 0.862$	ZZ	ZX	XZ	XX
Sent	5000000000	5000000000	5000000000	5000000000
n	6213134	6254960	6257058	6214725
n^L	6196831	6238602	6240697	6198420
n^U	6229523	6271404	6273505	6231116
m	30733	3123979	3127472	31031
m^L	29596	3112422	3115908	29888
m^U	31961	3135623	3139122	32264
Q	1.24×10^{-3}	1.25×10^{-3}	1.25×10^{-3}	1.24×10^{-3}
E	0.49%	49.94%	49.98%	0.50%
$\nu = 0.002$	ZZ	ZX	XZ	XX
Sent	5000000000	5000000000	5000000000	5000000000
n	14332	13771	14029	14362
n^L	13559	13013	13264	13588
n^U	15199	14622	14888	15230
m	64	6883	7099	78
m^L	23	6350	6558	31
m^U	142	7513	7738	162
Q	2.87×10^{-6}	2.75×10^{-6}	2.81×10^{-6}	2.87×10^{-6}
E	0.44%	49.98%	50.60%	0.54%
$\omega = 0.001$	ZZ	ZX	XZ	XX
Sent	5000000000	5000000000	5000000000	5000000000
n	7209	7178	7186	7208
n^L	6663	6634	6641	6662
n^U	7852	7820	7828	7851
m	40	3498	3699	48
m^L	11	3121	3311	15
m^U	109	3978	4190	120
Q	1.44×10^{-6}	1.44×10^{-6}	1.44×10^{-6}	1.44×10^{-6}
E	0.55%	48.72%	51.46%	0.66%

TABLE VII. Experimental data of BB84 in the standard case ($\theta = 0$).

$\mu = 0.866$	ZZ	ZX	XZ	XX
Sent	5000000000	5000000000	5000000000	5000000000
n	6210291	6342552	6326748	6211741
n^L	6193992	6326080	6310296	6195440
n^U	6226676	6359110	6343286	6228128
m	26636	3243691	3059736	25527
m^L	25578	3231914	3048298	24491
m^U	27785	3255554	3071260	26654
Q	1.24×10^{-3}	1.27×10^{-3}	1.27×10^{-3}	1.24×10^{-3}
E	0.43%	51.14%	48.36%	0.41%
$\nu = 0.002$	ZZ	ZX	XZ	XX
Sent	5000000000	5000000000	5000000000	5000000000
n	14439	14498	14408	14545
n^L	13663	13720	13633	13766
n^U	15309	15369	15277	15418
m	59	7234	7265	85
m^L	20	6687	6717	35
m^U	136	7878	7910	171
Q	2.89×10^{-6}	2.90×10^{-6}	2.88×10^{-6}	2.91×10^{-6}
E	0.41%	49.89%	50.42%	0.58%
$\omega = 0.001$	ZZ	ZX	XZ	XX
Sent	5000000000	5000000000	5000000000	5000000000
n	7286	7282	7288	7295
n^L	6737	6734	6739	6746
n^U	7932	7927	7934	7941
m	25	3632	3677	34
m^L	5	3248	3290	8
m^U	86	4119	4167	100
Q	1.46×10^{-6}	1.46×10^{-6}	1.46×10^{-6}	1.46×10^{-6}
E	0.34%	49.87%	50.44%	0.46%

TABLE VIII. Experimental data of DB-QKD in the misaligned case with $\theta = \pi/9$.

$\mu = 0.529$	ZZ	ZX	XZ	XX
Sent	5000000000	5000000000	5000000000	5000000000
n	3797640	3868733	3857618	3801354
n^L	3784896	3855870	3844774	3788604
n^U	3810470	3881682	3870548	3814190
m	91409	2597132	1246715	101024
m^L	89440	2586595	1239418	98954
m^U	93466	2607755	1254099	103182
Q	7.60×10^{-4}	7.74×10^{-4}	7.72×10^{-4}	7.60×10^{-4}
E	2.41%	67.13%	32.32%	2.66%
$\nu = 0.002$	ZZ	ZX	XZ	XX
Sent	5000000000	5000000000	5000000000	5000000000
n	14411	14524	14356	14409
n^L	13635	13745	13582	13634
n^U	15280	15396	15223	15278
m	310	9487	5022	348
m^L	204	8860	4568	236
m^U	636	10210	5576	662
Q	2.88×10^{-6}	2.90×10^{-6}	2.87×10^{-6}	2.88×10^{-6}
E	2.15%	65.31%	34.98%	2.41%
$\omega = 0.001$	ZZ	ZX	XZ	XX
Sent	5000000000	5000000000	5000000000	5000000000
n	7240	7279	7284	7238
n^L	6693	6731	6736	6691
n^U	7884	7924	7930	7882
m	153	4823	2457	163
m^L	82	4379	2143	89
m^U	1131	5368	2879	916
Q	1.45×10^{-6}	1.46×10^{-6}	1.46×10^{-6}	1.45×10^{-6}
E	2.11%	66.24%	33.73%	2.25%

TABLE IX. Experimental data of BB84 in the misaligned case with $\theta = \pi/9$.

$\mu = 0.483$	ZZ	ZX	XZ	XX
Sent	5000000000	5000000000	5000000000	5000000000
n	3480616	3348746	3334788	3393023
n^L	3468416	3336780	3322847	3380978
n^U	3492902	3360798	3346815	3405154
m	95459	2241204	1152243	99148
m^L	93447	2231416	1145228	97097
m^U	97559	2251078	1159344	101287
Q	6.96×10^{-4}	6.70×10^{-4}	6.67×10^{-4}	6.79×10^{-4}
E	2.74%	66.93%	34.55%	2.92%
$\nu = 0.002$	ZZ	ZX	XZ	XX
Sent	5000000000	5000000000	5000000000	5000000000
n	14417	14466	14537	14448
n^L	13641	13689	13758	13671
n^U	15286	15336	15409	15318
m	682	9578	4913	484
m^L	521	8948	4464	350
m^U	986	10304	5462	783
Q	2.88×10^{-6}	2.89×10^{-6}	2.91×10^{-6}	2.89×10^{-6}
E	4.72%	66.21%	33.79%	3.35%
$\omega = 0.001$	ZZ	ZX	XZ	XX
Sent	5000000000	5000000000	5000000000	5000000000
n	7410	7351	7402	7475
n^L	6857	6800	6849	6919
n^U	8060	7999	8052	8128
m	389	4975	2449	188
m^L	270	4523	2135	108
m^U	695	5526	2871	711
Q	1.48×10^{-6}	1.47×10^{-6}	1.48×10^{-6}	1.50×10^{-6}
E	5.25%	67.67%	33.08%	2.50%

TABLE X. Experimental data of DB-QKD in the misaligned case with $\theta = 2\pi/9$.

$\mu = 0.185$	<i>ZZ</i>	<i>ZX</i>	<i>XZ</i>	<i>XX</i>
Sent	5000000000	5000000000	5000000000	5000000000
<i>n</i>	1357439	1336403	1324516	1346323
n^L	1349824	1328847	1316994	1338739
n^U	1365140	1344045	1332124	1353993
<i>m</i>	163682	1078092	256855	175220
m^L	161044	1071307	253548	172491
m^U	166407	1084964	260249	178037
<i>Q</i>	2.71×10^{-4}	2.67×10^{-4}	2.65×10^{-4}	2.69×10^{-4}
<i>E</i>	12.06%	80.67%	19.39%	13.01%
$\nu = 0.002$	<i>ZZ</i>	<i>ZX</i>	<i>XZ</i>	<i>XX</i>
Sent	5000000000	5000000000	5000000000	5000000000
<i>n</i>	14446	14265	14349	14438
n^L	13670	13493	13575	13662
n^U	15316	15130	15216	15308
<i>m</i>	1370	11416	2896	1397
m^L	1138	10727	2554	1162
m^U	1721	12200	3344	1750
<i>Q</i>	2.89×10^{-6}	2.85×10^{-6}	2.87×10^{-6}	2.89×10^{-6}
<i>E</i>	9.48%	80.02%	20.18%	9.68%
$\omega = 0.001$	<i>ZZ</i>	<i>ZX</i>	<i>XZ</i>	<i>XX</i>
Sent	5000000000	5000000000	5000000000	5000000000
<i>n</i>	7277	7251	7259	7266
n^L	6729	6704	6712	6718
n^U	7922	7895	7904	7911
<i>m</i>	688	5857	1398	700
m^L	526	5366	1163	537
m^U	992	6446	1751	1005
<i>Q</i>	1.46×10^{-6}	1.45×10^{-6}	1.45×10^{-6}	1.45×10^{-6}
<i>E</i>	9.44%	80.75%	19.25%	9.63%

TABLE XI. Experimental data of DB-QKD in the general case.

$\mu = 0.631$	ZZ	ZX	XZ	XX
Sent	20000000000	20000000000	20000000000	20000000000
n	18217672	18242614	18311809	18233143
n^L	18189748	18214671	18283813	18205207
n^U	18245682	18270643	18339891	18261165
m	369969	10665685	7640707	323117
m^L	365998	10644321	7622627	319407
m^U	374027	10687135	7658873	326914
Q	9.11×10^{-4}	9.12×10^{-4}	9.16×10^{-4}	9.12×10^{-4}
E	2.03%	58.47%	41.73%	1.77%
$\nu = 0.002$	ZZ	ZX	XZ	XX
Sent	20000000000	20000000000	20000000000	20000000000
n	58106	57858	57947	58340
n^L	56539	56294	56382	56769
n^U	59763	59511	59602	60000
m	1034	33737	24243	1086
m^L	833	32545	23234	880
m^U	1361	35019	25343	1416
Q	2.91×10^{-6}	2.89×10^{-6}	2.90×10^{-6}	2.92×10^{-6}
E	1.78%	58.31%	41.84%	1.86%
$\omega = 0.001$	ZZ	ZX	XZ	XX
Sent	20000000000	20000000000	20000000000	20000000000
n	29080	29156	29157	29102
n^L	27974	28049	28050	27996
n^U	30277	30354	30355	30299
m	709	16905	12110	603
m^L	545	16064	11400	452
m^U	1014	17839	12914	903
Q	1.45×10^{-6}	1.46×10^{-6}	1.46×10^{-6}	1.46×10^{-6}
E	2.44%	57.98%	41.53%	2.07%

- [1] E. Chitambar and G. Gour, *Reviews of Modern Physics* **91**, 025001 (2019).
- [2] C. H. Bennett and G. Brassard, in *Proceedings of IEEE International Conference on Computers, Systems and Signal Processing* (IEEE, 1984) pp. 175–179.
- [3] A. K. Ekert, *Physical review letters* **67**, 661 (1991).
- [4] P. W. Shor and J. Preskill, *Physical review letters* **85**, 441 (2000).
- [5] C. Gobby, Z. Yuan, and A. Shields, *Applied Physics Letters* **84**, 3762 (2004).
- [6] R. Renner, *International Journal of Quantum Information* **6**, 1 (2008).
- [7] H.-K. Lo, M. Curty, and B. Qi, *Physical review letters* **108**, 130503 (2012).
- [8] M. Lucamarini, Z. L. Yuan, J. F. Dynes, and A. J. Shields, *Nature* **557**, 400 (2018).
- [9] V. Scarani, H. Bechmann-Pasquinucci, N. J. Cerf, M. Dušek, N. Lütkenhaus, and M. Peev, *Reviews of modern physics* **81**, 1301 (2009).
- [10] H.-K. Lo, M. Curty, and K. Tamaki, *Nature Photonics* **8**, 595 (2014).
- [11] S. Pirandola, U. L. Andersen, L. Banchi, M. Berta, D. Bunandar, R. Colbeck, D. Englund, T. Gehring, C. Lupo, C. Ottaviani, *et al.*, *Advances in optics and photonics* **12**, 1012 (2020).
- [12] F. Xu, X. Ma, Q. Zhang, H.-K. Lo, and J.-W. Pan, *Reviews of Modern Physics* **92**, 025002 (2020).
- [13] D. Mayers and A. Yao, in *Proceedings 39th Annual Symposium on Foundations of Computer Science (Cat. No. 98CB36280)* (IEEE, 1998) pp. 503–509.
- [14] K. Horodecki, M. Horodecki, P. Horodecki, and J. Oppenheim, *Physical review letters* **94**, 160502 (2005).
- [15] A. Acín, N. Gisin, and L. Masanes, *Physical review letters* **97**, 120405 (2006).
- [16] A. Acín, N. Brunner, N. Gisin, S. Massar, S. Pironio, and V. Scarani, *Physical Review Letters* **98**, 230501 (2007).
- [17] S. Pironio, A. Acín, N. Brunner, N. Gisin, S. Massar, and V. Scarani, *New Journal of Physics* **11**, 045021 (2009).
- [18] S. Pirandola, *Scientific reports* **4**, 1 (2014).
- [19] H. Ollivier and W. H. Zurek, *Physical review letters* **88**, 017901 (2001).
- [20] K. Modi, A. Brodutch, H. Cable, T. Paterek, and V. Vedral, *Reviews of Modern Physics* **84**, 1655 (2012).
- [21] R. Wang, Y. Yao, Z.-Q. Yin, and H.-K. Lo, *arXiv preprint arXiv:2303.11167* (2023).
- [22] K. Tamaki, M. Curty, G. Kato, H.-K. Lo, and K. Azuma, *Physical Review A* **90**, 052314 (2014).
- [23] Z.-Q. Yin, C.-H. F. Fung, X. Ma, C.-M. Zhang, H.-W. Li,

- W. Chen, S. Wang, G.-C. Guo, and Z.-F. Han, *Physical Review A* **88**, 062322 (2013).
- [24] Z.-Q. Yin, C.-H. F. Fung, X. Ma, C.-M. Zhang, H.-W. Li, W. Chen, S. Wang, G.-C. Guo, and Z.-F. Han, *Physical Review A* **90**, 052319 (2014).
- [25] L. Henderson and V. Vedral, *Journal of physics A: mathematical and general* **34**, 6899 (2001).
- [26] J. Bowles, M. T. Quintino, and N. Brunner, *Physical review letters* **112**, 140407 (2014).
- [27] N. J. Beaudry, T. Moroder, and N. Lütkenhaus, *Physical review letters* **101**, 093601 (2008).
- [28] C.-H. F. Fung, H. Chau, and H.-K. Lo, *Physical Review A* **84**, 020303 (2011).
- [29] W.-Y. Hwang, *Physical Review Letters* **91**, 057901 (2003).
- [30] H.-K. Lo, X. Ma, and K. Chen, *Physical review letters* **94**, 230504 (2005).
- [31] X.-B. Wang, *Physical review letters* **94**, 230503 (2005).
- [32] X. Ma, B. Qi, Y. Zhao, and H.-K. Lo, *Physical Review A* **72**, 012326 (2005).
- [33] S. M. Barnett and S. J. Phoenix, *Journal of Modern Optics* **40**, 1443 (1993).
- [34] M. Koashi, *New Journal of Physics* **11**, 045018 (2009).
- [35] F. Buscemi, M. Keyl, G. M. D'Ariano, P. Perinotti, and R. F. Werner, *Journal of mathematical physics* **46**, 082109 (2005).
- [36] G. M. D'Ariano, P. L. Presti, and P. Perinotti, *Journal of Physics A: Mathematical and General* **38**, 5979 (2005).
- [37] E. Haapasalo, T. Heinosaari, and J.-P. Pellonpää, *Quantum Information Processing* **11**, 1751 (2012).
- [38] M. Oszmaniec, L. Guerini, P. Wittek, and A. Acín, *Physical review letters* **119**, 190501 (2017).
- [39] D. Gottesman, H.-K. Lo, N. Lutkenhaus, and J. Preskill, in *International Symposium on Information Theory, 2004. ISIT 2004. Proceedings.* (IEEE, 2004) p. 136.
- [40] R. Horodecki and P. Horodecki, *Physics Letters A* **210**, 227 (1996).
- [41] R. Horodecki *et al.*, *Physical Review A* **54**, 1838 (1996).
- [42] M. Koashi and A. Winter, *Physical Review A* **69**, 022309 (2004).
- [43] I. Devetak and A. Winter, *Proceedings of the Royal Society A: Mathematical, Physical and engineering sciences* **461**, 207 (2005).
- [44] S. Wang, W. Chen, Z.-Q. Yin, D.-Y. He, C. Hui, P.-L. Hao, G.-J. Fan-Yuan, C. Wang, L.-J. Zhang, J. Kuang, *et al.*, *Optics letters* **43**, 2030 (2018).
- [45] M. Christandl, R. König, and R. Renner, *Physical review letters* **102**, 020504 (2009).
- [46] X.-B. Wang, *Physical Review A* **75**, 052301 (2007).
- [47] K. Yoshino, M. Fujiwara, K. Nakata, T. Sumiya, T. Sasaki, M. Takeoka, M. Sasaki, A. Tajima, M. Koashi, and A. Tomita, *npj Quantum Information* **4**, 1 (2018).
- [48] A. Mizutani, G. Kato, K. Azuma, M. Curty, R. Ikuta, T. Yamamoto, N. Imoto, H.-K. Lo, and K. Tamaki, *npj Quantum Information* **5**, 1 (2019).
- [49] F.-Y. Lu, X. Lin, S. Wang, G.-J. Fan-Yuan, P. Ye, R. Wang, Z.-Q. Yin, D.-Y. He, W. Chen, G.-C. Guo, *et al.*, *npj Quantum Information* **7**, 1 (2021).
- [50] Z. Cao, Z. Zhang, H.-K. Lo, and X. Ma, *New Journal of Physics* **17**, 053014 (2015).
- [51] L. Liu, Y. Wang, E. Lavie, C. Wang, A. Ricou, F. Z. Guo, and C. C. W. Lim, *Physical Review Applied* **12**, 024048 (2019).
- [52] I. W. Primaatmaja, E. Lavie, K. T. Goh, C. Wang, and C. C. W. Lim, *Physical Review A* **99**, 062332 (2019).
- [53] L. Lydersen, C. Wiechers, C. Wittmann, D. Elser, J. Skaar, and V. Makarov, *Nature photonics* **4**, 686 (2010).
- [54] N. Gisin, S. Fasel, B. Kraus, H. Zbinden, and G. Ribordy, *Physical Review A* **73**, 022320 (2006).
- [55] P. Busch, P. Lahti, J.-P. Pellonpää, and K. Ylino, *Quantum measurement*, Vol. 23 (Springer, 2016).
- [56] O. Gühne, E. Haapasalo, T. Kraft, J.-P. Pellonpää, and R. Uola, *Reviews of Modern Physics* **95**, 011003 (2023).
- [57] A. Datta, *Studies on the role of entanglement in mixed-state quantum computation* (The University of New Mexico, 2008).
- [58] S. Luo, *Physical Review A* **77**, 042303 (2008).
- [59] M. D. Lang and C. M. Caves, *Physical review letters* **105**, 150501 (2010).
- [60] Z. Zhang, Q. Zhao, M. Razavi, and X. Ma, *Physical Review A* **95**, 012333 (2017).
- [61] A. Streltsov, H. Kampermann, and D. Bruß, *Physical review letters* **107**, 170502 (2011).